



A directional framework of similarity laws for geometrically distorted structures subjected to impact loads

Shuai Wang ^{a,b}, Fei Xu ^{a,b,*}, Xiaoyu Zhang ^{a,b}, Zhen Dai ^{a,b}, Xiaochuan Liu ^c, Chunyu Bai ^c

^a School of Aeronautics, Northwestern Polytechnical University, Xi'an 710072, Shaanxi, China;

^b Institute for Computational Mechanics and Its Applications, Northwestern Polytechnical University, Xi'an 710072, Shaanxi, China;

^c Aviation Key Laboratory of Science and Technology on Structures Impact Dynamics, Aircraft Strength Research Institute of China, Xi'an 710065, China



ARTICLE INFO

Keywords:
 Dimension
 Similarity
 Scaling
 Geometric distortion
 Response number
 Structural impact

ABSTRACT

A directional framework of similarity laws, termed oriented-density-length-velocity (ODLV) system, is suggested for the geometrically distorted structures subjected to impact loads. The distinct feature of the framework is that the newly proposed oriented dimensions, dimensionless numbers and scaling factors for all basic physical quantities are explicitly expressed by three characteristic lengths of spatial directions, which overcomes the inherent defects only with one scalar length in the traditional dimensional analysis. Meanwhile, similarity laws of the directional stresses, strains and displacements are expressed by different power law relationships of the ratios of undistorted characteristic lengths to distorted characteristic lengths. Therefore, the ability of similarity theory to express structural geometric characteristics are effectively developed. Based on the newly proposed framework, the non-scalabilities of geometric and material distortion (including strain hardening and strain rate effects) and the gravity effects could be compensated by correction methods of velocity, density and geometry. The analytical models of beams subjected to impact mass and impulsive velocity are verified. The results show that the proposed framework has excellent performance for expressing various dimensionless response equations and geometrically distorted scaling. A numerical model of circular plate subjected to dynamic pressure pulse is further carried out to verify the geometrically distorted scaling of the directional components of displacement, strain and stress. The refined analysis results show that, structural dimensionless responses in different directions can behave good consistency between the scaled model and the prototype in both the spatial and the temporal fields, with the correction of the directional physical quantities using different powers of the ratios of characteristic lengths.

1. Introduction

Although great achievements for structures subjected to impact loads have been made in theoretical and numerical researches, the analysis results without experimental verification are usually difficult to be accepted [1]. As an attractive important approach, the testing of a scaled model instead of the full-size prototype has a great advantage due to low economic cost, short period and simple experimental conditions [2,3], especially for large structures such as aircrafts, ships and trains. The methodology relating the scaled model and full-size prototype, termed as similarity laws, usually contains the similarity of geometry, kinetics, kinematics and constitutive relation in the mechanical system [4,5]. As a most important premise of the similarity laws, the geometric similarity usually requires that the characteristic lengths of three spatial directions

(i.e., \bar{L}_x , \bar{L}_y and \bar{L}_z for the Cartesian coordinate system (x, y, z) , where \bar{L} represents scalar characteristic length) should have the same basic scaling factor $\beta_{\bar{L}}$. In general, $\beta_{\bar{L}}$ can be called as geometrically-similar scaling factor and defined as $\beta_{\bar{L}} = \bar{L}_m / \bar{L}_p$, where β is the scaling factor; the subscripts m and p represent the scaled model and the full-size prototype, respectively.

The classical similarity laws, based on identical materials and pure geometrical scaling between scaled model and prototype, have long been known and systematically summarized by Jones [6]. In that work, a framework containing twenty-two dimensionless numbers, obtained by scalar dimensional analysis of the mass-length-time (MLT) bases, was proposed as the theoretical basis of similarity laws. The basic geometrically-similar scaling factor $\beta_{\bar{L}}$ was used to relate various physical quantities, as shown in Table 1. However, it must be used with great

* Corresponding author.

E-mail address: xufei@nwpu.edu.cn (F. Xu).

Table 1
Main scaling factors in MLT.

Variable	Scaling factor	Variable	Scaling factor
Length, \bar{L}	$\beta_{\bar{L}} = \bar{L}_m/\bar{L}_p$	Displacement, δ	$\beta_{\delta} = \beta_{\bar{L}}$
Density, ρ	$\beta_{\rho} = 1$	Stress, σ	$\beta_{\sigma} = 1$
Velocity, V	$\beta_V = 1$	Strain, ϵ	$\beta_{\epsilon} = 1$
Mass, m	$\beta_m = \beta_{\bar{L}}^3$	Strain rate, $\dot{\epsilon}$	$\beta_{\dot{\epsilon}} = 1/\beta_{\bar{L}}$
Time, t	$\beta_t = \beta_{\bar{L}}$	Acceleration, A	$\beta_A = 1/\beta_{\bar{L}}$

Table 2
Main scaling factors in VSG.

Variable	Scaling factor	Variable	Scaling factor
Length, \bar{L}	$\beta_{\bar{L}} = \bar{L}_m/\bar{L}_p$	Displacement, δ	$\beta_{\delta} = \beta_{\bar{L}}$
Density, ρ	$\beta_{\rho} = \rho_m/\rho_p$	Stress, σ	$\beta_{\sigma} = \beta_{\rho}\beta_V^2$
Velocity, V	$\beta_V = V_m/V_p$	Strain, ϵ	$\beta_{\epsilon} = 1$
Mass, m	$\beta_m = \beta_{\rho}\beta_{\bar{L}}^3$	Strain rate, $\dot{\epsilon}$	$\beta_{\dot{\epsilon}} = \beta_V/\beta_{\bar{L}}$
Time, t	$\beta_t = \beta_{\bar{L}}/\beta_V$	Acceleration, A	$\beta_A = \beta_V^2/\beta_{\bar{L}}$

Table 3
Main scaling factors in VSM.

Variable	Scaling factor	Variable	Scaling factor
Dimension, χ ^a	β_{χ}	Acceleration, A	$\beta_A = \beta_H^2\beta_{\sigma_d}/\beta_M$
Density, ρ	$\beta_{\rho} = \rho_m/\rho_p$	Displacement, δ_{χ}	$\beta_{\delta_{\chi}} = \beta_{\chi}$
Velocity, V	$\beta_V = (\beta_H^3\beta_{\sigma_d}/\beta_M)^{1/2}$	Stress, σ	$\beta_{\sigma} = \beta_{\sigma_d}$
Impact mass, G	$\beta_G = \beta_M$ ^b	Strain, ϵ	$\beta_{\epsilon} = 1$
Time, t	$\beta_t = \beta_{\chi}/\beta_V$	Strain rate, $\dot{\epsilon}$	$\beta_{\dot{\epsilon}} = \beta_V/\beta_H$

^a χ denotes a general direction.

^b For beams and plates with half length L , $\beta_M = \beta_{\rho}\beta_{\bar{L}}^2\beta_H$; for circular plates with radius R , $\beta_M = \beta_{\rho}\beta_R^2\beta_H$.

care because the primary premise of geometrically-similar scaling was easily broken, especially for the scaling of the thickness direction of thin-walled structures. For a scaled model, if one or more of the characteristic lengths of the spatial directions does not satisfy the factor $\beta_{\bar{L}}$, it is called geometric distortion.

In addition to the geometric distortion, some other distortions caused by materials, gravity effects and fracture could also result in invalidation of the scaling relations in Table 1 [6–12]. For the scaled experiments of impacted tubes, Drazetic et al. [13] proposed a scaling technique correcting the initial conditions to address the distortion of material strain-rate-sensitivity. Oshiro and Alves [14–16] proposed a scalar dimensional analysis based on the initial impact velocity V_0 - dynamic flow stress σ_d - impact mass G (VSG) to compensate for the distortion of material strain-rate-sensitivity in the general impact problems. On the basis of the geometrically-similar scaling factor $\beta_{\bar{L}}$, one more basic factor β_V was used to reasonably correct the impact velocity of the scaled model. By further adding the basic density factor β_{ρ} in the VSG, the impact mass and the structural mass of the scaled model were also corrected to compensate for the distortion of different materials in density, yield stress and strain-rate-sensitivity [17–20] and the distortion of gravity effects [21]. The solutions of material distortion, further including the distortions of strain hardening effects and fracture, were verified by a group of transport equations in continuum mechanics in the work of Sadeghi et al. [22–24]. In summary, the above studies established a new framework of VSG similarity laws: (1) the three basic factors $\beta_{\bar{L}}$, β_V and β_{ρ} were used to relate various physical quantities, as shown in Table 2; (2) the initial conditions of the scaled model were reasonably corrected by the factors β_V and β_{ρ} to compensate for the distortion of materials, gravity effects and fracture.

Although effectively extending scaling ability of the classical similarity laws, for the scaled model with geometric distortion, the VSG was still invalid due to its primary premise of geometrically-similar scaling. Based on the VSG system, Oshiro and Alves [25] presented an indirect empirical method in which the iterative scaling tests were used to determine the unknown scaling relations of geometric distortion. However, the indirect method cannot be practical for a wide range of applications due to its obvious defects that it works based on the experience of researchers and the numerous tests [26]. Through the velocity-dynamic flow stress-structure mass (VSM) dimensional analysis instead of the VSG system, Mazzariol and Alves [27,28] presented a direct scaling method for the impacted beams and plates to overcome the defects of the indirect empirical method. However, since the VSM is essentially a scalar dimensional analysis without the base of structural characteristic lengths, it is very difficult to express similarity laws of geometric distortion fundamentally and comprehensively. The above difficulties formed the basic motivation for further development of new dimensional analysis framework in this paper.

The major criticism for the above similarity laws is that all of them were impeded in essence by the premise of the geometrically-similar scaling, which motivates Wang, Xu and Dai [29] to suggest a similarity laws of the density-length-velocity (DLV) bases. Not only does the DLV system has the exactly same scaling relations with the Table 2, but it also has the essential superiority in expressing the well-known Johnson's damage number D_n ¹, the well-known Zhao's response number R_n ² and the various dimensionless response equations of structural impact. More importantly, to overcome the difficulty of geometric distortion reasonably and systematically, it is easy to be extended from the base of scalar characteristic length \bar{L} to the base of three spatial directional characteristic lengths \bar{L}_x , \bar{L}_y and \bar{L}_z in dimensional analysis in the present paper. The new directional framework of similarity laws shows more superiority over the previous dimensional analysis systems.

In what follows, Section 2 introduces our newly proposed framework of similarity laws. Section 3 investigates the analytical models of various beams subjected to impact mass and impulsive velocity. Section 4 investigates a numerical model of circular plate subjected to dynamic pressure pulse. Section 5 summarizes this work.

2. The directional framework of similarity laws

2.1. A brief review of the previous work

When considering geometrically distorted structures, the previous similarity laws could not work due to the unsatisfaction of primary premise that required the same geometric scaling factor $\beta_{\bar{L}}$ for the characteristic lengths of structures in different directions. To remedy the invalidation of similarity laws, Oshiro and Alves [25] defined a geometric distortion factor $\beta_i = (\beta_{\bar{L}_i}/\beta_{\bar{L}})^{n_i}$ for the distorted characteristic length \bar{L}_i and the physical quantity i . Then, an indirect empirical method (see Ref. [25]) is proposed to iteratively determine the unknown exponent n_i . However, as pointed out in Section 1, this method cannot be practical for a wide range of applications due to completely dependents

¹ The Johnson's damage number [6,30,31] is defined as $D_n = \frac{\rho V_0^2}{\sigma_0}$ and is used to measure the order of strain imposed in various impact regions of a structure, where σ_0 is static flow stress.

² The Zhao's response number [32–36] is defined as $R_n(n) = \frac{\rho V_0^2}{\sigma_0} \left(\frac{\bar{L}}{H}\right)^2, \frac{\rho V_0^2}{\sigma_0} \left(\frac{\bar{L}}{\bar{L}'}\right)^n, \frac{\rho V_0^2}{E} \left(\frac{\bar{L}}{\bar{L}'}\right)^n$, et al and is used to control the response of simple impacted structures, where H is the geometrical thickness of beam, plate, et al., \bar{L}' is characteristic lengths of other-directions, E is Young's modulus/shear modulus, n was a real number. In general, the response number $R_n(n)$ can be seen as a combination of the dimensionless stress ($\rho V_0^2/\sigma_0$) and the dimensionless characteristic length (\bar{L}/H).

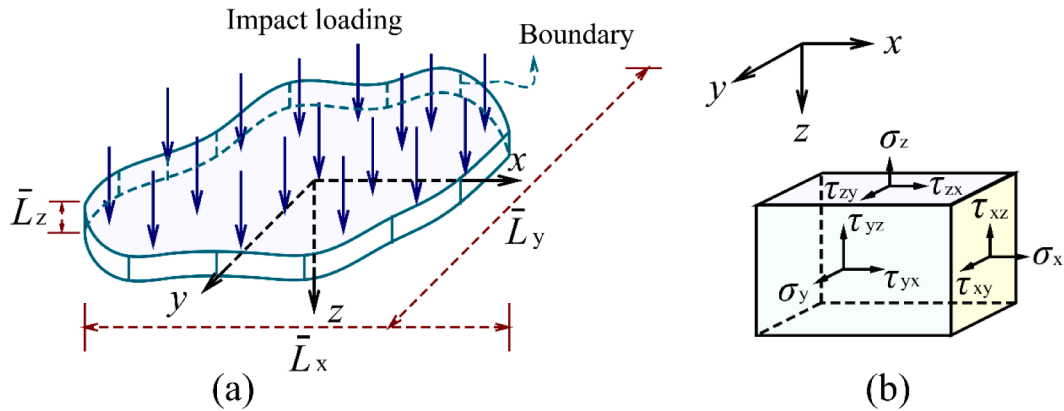


Fig. 1. Impact model of thin-plate problem. (a) Thin-plate subjected to transverse impact loads. (b) Schematic diagram of directions and subscripts of stress components.

on the experience of researchers and the numerous tests.

Recently, Mazzariol and Alves [27,28] further presented a direct geometrically-distorted method based on a scalar dimensional analysis of the VSM. In the work, eight dimensionless numbers for beams and plates were proposed to derive the main scaling factors, as shown in Table 3. The characteristic lengths of three spatial directions were indirectly introduced by the structural mass, i.e. $\beta_M = \beta_\rho \beta_L^2 \beta_H$ (or $\beta_M = \beta_\rho \beta_R^2 \beta_H$). As a consequence, six basic factors β_x , β_{σ_d} , β_M , β_H , β_{V_x} and β_p formed the scaling relations of geometric distortion of thickness (i.e., $\beta_H \neq \beta_L$ or $\beta_H \neq \beta_R$).

Compared with the indirect empirical method, it is evident from Table 3 that the scaling factors for geometric distortion of thickness are explicitly expressed. Nevertheless, since the VSM is essentially a scalar dimensional analysis, three main defects were easily found: (1) The characteristic lengths of spatial directions were introduced through a scalar of structural mass M , resulting in serious theoretical defects in mathematics; (2) The scaling factor $\beta_e = 1$ was contradictory to the geometric distortion since the distortion means the geometrically-similar scaling of structural deformation was broken; (3) The directional physical quantities such as components of the stress, strain and displacement were not systematically expressed in Table 3. Therefore, the VSM has no ability to express the similarity laws of geometric distortion objectively and completely.

Since the capability of the indirect empirical method and the VSM system for geometric distortion is very limited, it is imperative to expand the previous similarity laws to overcome the limitation of the scalar characteristic length and the single geometric scaling factor.

2.2. Oriented dimensions

To further expand the capability of dimensional analysis to express geometric distortion, three oriented length dimensions \mathbb{L}_x , \mathbb{L}_y and \mathbb{L}_z [37, 38] for the three directional characteristic lengths \bar{L}_x , \bar{L}_y and \bar{L}_z are used instead of one scalar length dimension \mathbb{L} of all previous researches. Although the concept of oriented dimension was put forward very early in Refs. [37] and [38], these works have hardly applied it to the problems of solid mechanics. Then, the five basic dimensions \mathbb{M} , \mathbb{L}_x , \mathbb{L}_y , \mathbb{L}_z and \mathbb{T} form the bases of oriented dimensional analysis in the solid mechanic system, where the symbols \mathbb{M} and \mathbb{T} represents dimensions of the mass m and the time t , respectively. As a convenience, the notation ' $\text{dim}()$ ' is used to represent the dimension; for instance, $\text{dim}(\bar{L}_x) = \mathbb{L}_x$.

To determine the main physical quantities of similarity laws, impact problem of a thin-plate subjected to transverse impact loads is given, as shown in Fig. 1. The thin-plate impact problem is assumed to be an initial flat thin-plate with the arbitrary shape and boundary conditions in the cartesian coordinate system (x, y, z) , Fig. 1a. The directions and

subscripts of physical quantities are shown in stress components on an infinitesimal rectangular element, Fig. 1b. It should be noted that the symbol τ specifically refers to shear stress and has the relations $\tau_{xy} = \sigma_{xy}$, $\tau_{xz} = \sigma_{xz}$ and $\tau_{yz} = \sigma_{yz}$.

- Impact loads

Dimension of three kinds of transverse impact loads is considered as: (1) impact velocity V_z , $\text{dim}(V_z) = \mathbb{L}_z \mathbb{T}^{-1}$; (2) impact mass G , $\text{dim}(G) = \mathbb{M}$; (3) impulse pressure P_z , $\text{dim}(P_z) = \text{dim}(\sigma_z)$; and its loading time t_f , $\text{dim}(t_f) = \mathbb{T}$.

- Kinetics

For the normal stress $\sigma_x = \lim_{\Delta S_{yz} \rightarrow 0} (\Delta F_x / \Delta S_{yz})$ with F and S being force and area, respectively, $\text{dim}(\sigma_x) = (\mathbb{M} \mathbb{L}_x \mathbb{T}^{-2})(\mathbb{L}_y \mathbb{L}_z)^{-1} = \mathbb{L}_x \mathbb{L}_y^{-1} \mathbb{L}_z^{-1} \mathbb{M} \mathbb{T}^{-2}$. Similarly, the oriented dimensions of σ_y , σ_z , τ_{xy} , τ_{xz} and τ_{yz} can be derived as $\mathbb{L}_x^{-1} \mathbb{L}_y \mathbb{L}_z^{-1} \mathbb{M} \mathbb{T}^{-2}$, $\mathbb{L}_x^{-1} \mathbb{L}_y^{-1} \mathbb{L}_z \mathbb{M} \mathbb{T}^{-2}$, $\mathbb{L}_z^{-1} \mathbb{M} \mathbb{T}^{-2}$, $\mathbb{L}_y^{-1} \mathbb{M} \mathbb{T}^{-2}$ and $\mathbb{L}_x^{-1} \mathbb{M} \mathbb{T}^{-2}$, respectively. It is easy to verify that, if $\text{dim}(\rho) = \mathbb{M} \mathbb{L}_x^{-1} \mathbb{L}_y^{-1} \mathbb{L}_z^{-1}$, $\text{dim}(\delta_x) = \mathbb{L}_x$, $\text{dim}(\delta_y) = \mathbb{L}_y$ and $\text{dim}(\delta_z) = \mathbb{L}_z$, the oriented dimensions of stress are satisfied for the equation of motion of a solid. For example, for the equation of motion in the x -direction $\frac{\partial \sigma_x}{\partial x} + \frac{\partial \tau_{xy}}{\partial y} + \frac{\partial \tau_{xz}}{\partial z} = \rho \frac{\partial^2 \delta_x}{\partial t^2}$ [39], the oriented relation $\frac{\text{dim}(\sigma_x)}{\mathbb{L}_x} + \frac{\text{dim}(\tau_{xy})}{\mathbb{L}_y} + \frac{\text{dim}(\tau_{xz})}{\mathbb{L}_z} = \text{dim}(\rho) \frac{\text{dim}(\delta_x)}{\mathbb{T}^2}$ is satisfied.

- Kinematics

The Green-Lagrange strain component along x -axis is expressed as $\epsilon_x = \frac{\partial \delta_x}{\partial x} + \frac{1}{2} \left[\left(\frac{\partial \delta_x}{\partial x} \right)^2 + \left(\frac{\partial \delta_y}{\partial x} \right)^2 + \left(\frac{\partial \delta_z}{\partial x} \right)^2 \right]$ [39]. When the oriented dimensions $\text{dim}(\delta_x) = \mathbb{L}_x$, $\text{dim}(\delta_y) = \mathbb{L}_y$ and $\text{dim}(\delta_z) = \mathbb{L}_z$ are used, the oriented analysis of the strain component, $\text{dim}(\epsilon_x) = \frac{\text{dim}(\delta_x)}{\text{dim}(x)} = \left(\frac{\text{dim}(\delta_x)}{\text{dim}(x)} \right)^2 = \left(\frac{\text{dim}(\delta_x)}{\text{dim}(x)} \right)^2 = \left(\frac{\text{dim}(\delta_x)}{\text{dim}(x)} \right)^2$, is not true.

To satisfy the dimensional homogeneity principle that all terms of an equation must have the same dimensions, the classical theory of thin-plate [39] is adopted. When the geometric nonlinearity belongs to small strains with the moderate rotations of transverse normal on the neutral plane (say $10^\circ - 15^\circ$), the nonlinear strain-displacement relations [39] take the following form

Table 4

Oriented dimensions of basic physical quantity in the thin-plate model.

Physical quantity	Dimension	Physical quantity	Dimension
Density ρ	$ML_x^{-1}L_y^{-1}L_z^{-1}$	Strain ϵ_z	1
Length L_x	L_x	Strain γ_{xz}	$L_x^{-1}L_z$
Length L_y	L_y	Strain γ_{yz}	$L_y^{-1}L_z$
Length L_z	L_z	Time t	T
Velocity V_z	$L_z T^{-1}$	Displacement δ_x	$L_x^{-1}L_z^2$
Stress σ_x	$L_x L_y^{-1} L_z^{-1} M T^{-2}$	Displacement δ_y	$L_y^{-1} L_z^2$
Stress σ_y	$L_x^{-1} L_y L_z^{-1} M T^{-2}$	Displacement δ_z	L_z
Stress σ_z	$L_x^{-1} L_y^{-1} L_z M T^{-2}$	Impact mass G	M
Stress τ_{xy}	$L_z^{-1} M T^{-2}$	Impulse pressure P_z	$L_x^{-1} L_y^{-1} L_z M T^{-2}$
Stress τ_{xz}	$L_y^{-1} M T^{-2}$	Equivalent stress σ_{eq}	$L_x^{-1} L_y L_z^{-1} M T^{-2}$
Stress τ_{yz}	$L_x^{-1} M T^{-2}$	Equivalent strain ϵ_{eq}	$L_x^{-2} L_z^2$
Strain ϵ_x	$L_x^{-2} L_z^2$	Plastic strain ϵ_z	$(L_x^{-2} L_z^2)^{mod}$
Strain ϵ_y	$L_y^{-2} L_z^2$	Plastic strain γ_{xz}	$(L_x^{-3} L_z^3)^{mod}$
Strain γ_{xy}	$L_x^{-1} L_y^{-1} L_z^2$	Plastic strain γ_{yz}	$(L_x^{-3} L_z^3)^{mod}$

$$\left. \begin{aligned} \epsilon_x &= \left\{ \frac{\partial \delta'_x}{\partial x} + \frac{1}{2} \left(\frac{\partial \delta'_z}{\partial x} \right)^2 \right\} + Z_0 \left\{ - \frac{\partial^2 \delta'_z}{\partial x^2} \right\} \\ \epsilon_y &= \left\{ \frac{\partial \delta'_y}{\partial y} + \frac{1}{2} \left(\frac{\partial \delta'_z}{\partial y} \right)^2 \right\} + Z_0 \left\{ - \frac{\partial^2 \delta'_z}{\partial y^2} \right\} \\ \gamma_{xy} &= \left\{ \frac{\partial \delta'_x}{\partial y} + \frac{\partial \delta'_y}{\partial x} + \frac{\partial \delta'_z}{\partial x} \frac{\partial \delta'_z}{\partial y} \right\} + Z_0 \left\{ - 2 \frac{\partial^2 \delta'_z}{\partial x \partial y} \right\} \\ \gamma_{xz} &= \left(- \frac{\partial \delta'_z}{\partial x} \right) + \left(\frac{\partial \delta'_z}{\partial x} \right), \quad \gamma_{yz} = \left(- \frac{\partial \delta'_z}{\partial y} \right) + \left(\frac{\partial \delta'_z}{\partial y} \right), \quad \epsilon_z = \frac{\partial \delta'_z}{\partial z} \end{aligned} \right\}, \quad (1a-f)$$

where δ' is the displacements of a material point on the neutral plane; Z_0 is the normal distance of the material point to the neutral plane; γ denotes shear strain specifically and $\gamma_{xy} = 2\epsilon_{xy}$, $\gamma_{xz} = 2\epsilon_{xz}$, $\gamma_{yz} = 2\epsilon_{yz}$. The terms in the first curly bracket of ϵ_x , ϵ_y and γ_{xy} in Eq. (1a-c) represent the membrane strains on the neutral planes; while the terms in the second curly bracket represent the bending strain from the curvatures. In the classical thin-plate theory, the transverse strains γ_{xz} , γ_{yz} and ϵ_z in Eq. (1d-f) are not taken into account.

In order to make Eq. (1a-f) meaningful, $\dim(\delta'_z)$ is taken to be the same dimension L_z with $\dim(\delta_z)$; while $\dim(\delta'_x)$ and $\dim(\delta'_y)$ can be accordingly modified as $L_x^{-1}L_z^2$ and $L_y^{-1}L_z^2$, respectively. Then, the oriented dimensions of ϵ_x , ϵ_y , γ_{xy} , γ_{xz} , γ_{yz} and ϵ_z are respectively derived as $L_x^{-2}L_z^2$, $L_y^{-2}L_z^2$, $L_x^{-1}L_y^{-1}L_z^2$, $L_x^{-1}L_z$, $L_y^{-1}L_z$ and 1. It is evident that $\dim(\delta_z) = L_z$, $\dim(\delta_x) = L_x^{-1}L_z^2$ and $\dim(\delta_y) = L_y^{-1}L_z^2$ are true for the whole displacement field of thin-plate, $\delta_x = \delta'_x - \left(Z_0 \frac{\partial \delta'_z}{\partial x} \right)$, $\delta_y = \delta'_y - \left(Z_0 \frac{\partial \delta'_z}{\partial y} \right)$ and $\delta_z = \delta'_z$.

• Equivalent stress and equivalent strain

For the assumptions of the thin-plate impact problem (ignoring transverse stress and strain components) and the isotropic rigid-plastic materials, the equivalent stress σ_{eq} and the equivalent strain ϵ_{eq} [40] can be reduced to

$$\sigma_{eq} = \sqrt{\sigma_x^2 + \sigma_y^2 - \sigma_x \sigma_y + 3\tau_{xy}^2}, \quad \epsilon_{eq} = \frac{2}{3} \sqrt{\epsilon_x^2 + \epsilon_y^2 - \epsilon_x \epsilon_y + 3\gamma_{xy}^2} \quad (2a-b)$$

The oriented analysis of Eq. (2) implies the inherent relations

$$\left. \begin{aligned} \dim(\sigma_{eq}) &= \dim(\sigma_x) = \dim(\sigma_y) = \dim(\sqrt{\sigma_x \sigma_y}) = \dim(\tau_{xy}) \\ \dim(\epsilon_{eq}) &= \dim(\epsilon_x) = \dim(\epsilon_y) = \dim(\sqrt{\epsilon_x \epsilon_y}) = \dim(\gamma_{xy}) \end{aligned} \right\} \quad (3a-b)$$

The directional homogeneity of Eq. (3) requires that the directions of L_x and L_y is not distinguished (or say that the x-y plane is isotropic). While, only the z direction of L_z and the in-plane directions of L_x and L_y are mutually independent. If the isotropic symbol L_{xy} is used instead of L_x and L_y , then $\dim(\sigma_{eq}) = L_{xy}^{-1} L_{xy} L_z^{-1} M T^{-2}$ and $\dim(\epsilon_{eq}) = L_{xy}^2 L_z^{-2}$ are obtained.

• Directional stress-strain relationship

The directional stress-strain relationship of the isotropic rigid-perfectly plastic model is further verified by the Le'yy – Mises theory [40]

$$\left. \begin{aligned} d\epsilon_x &= \frac{d\epsilon_{eq}}{\sigma_{eq}} \left[\sigma_x - \frac{1}{2} (\sigma_y + \sigma_z) \right], \quad d\epsilon_y = \frac{d\epsilon_{eq}}{\sigma_{eq}} \left[\sigma_y - \frac{1}{2} (\sigma_x + \sigma_z) \right], \\ d\epsilon_{xy} &= \frac{3}{2} \frac{d\epsilon_{eq}}{\sigma_{eq}} \tau_{xy}, \quad d\epsilon_{xz} = \frac{3}{2} \frac{d\epsilon_{eq}}{\sigma_{eq}} \tau_{xz}, \quad d\epsilon_{yz} = \frac{3}{2} \frac{d\epsilon_{eq}}{\sigma_{eq}} \tau_{yz}, \\ d\epsilon_z &= \frac{d\epsilon_{eq}}{\sigma_{eq}} \left[\sigma_z - \frac{1}{2} (\sigma_x + \sigma_y) \right] \end{aligned} \right\}, \quad (4a-f)$$

where $d\epsilon_x$, $d\epsilon_y$, $d\epsilon_{xy}$, $d\epsilon_{xz}$, $d\epsilon_{yz}$ and $d\epsilon_{eq}$ are the increments of six plastic strain components and equivalent plastic strain, respectively.

In the view of the thin-plate model that ignoring the transverse stress σ_z , it is easy to verify that the oriented dimensions of ϵ_x , ϵ_y , γ_{xy} , σ_x , σ_y , τ_{xy} and σ_{eq} , ϵ_{eq} are true for Eq. (4a-c).

In actual deformation, the transverse strain components are small but still exist. When the oriented dimensions of σ_{eq} , ϵ_{eq} , τ_{xz} , τ_{yz} , σ_x and σ_y are substituted into Eq. (4d-f), the oriented dimensions of γ_{xz} , γ_{yz} and ϵ_z are modified as $\dim(\gamma_{xz}) = \frac{\dim(\tau_{xz})}{\dim(\sigma_{eq})} \dim(\epsilon_{eq}) = (L_{xy}^{-3} L_z^3)^{mod}$, $\dim(\gamma_{yz}) = \frac{\dim(\tau_{yz})}{\dim(\sigma_{eq})} \dim(\epsilon_{eq}) = (L_{xy}^{-3} L_z^3)^{mod}$ and $\dim(\epsilon_z) = \dim(\epsilon_{eq}) = (L_{xy}^{-2} L_z^2)^{mod}$, respectively. So, for transverse strain components, the oriented dimensions are redefined by plastic stress-strain relationship. Since the modified dimensions of ϵ_z is same with $\dim(\epsilon_{eq})$, ϵ_z can be naturally included in the equivalent strain ϵ_{eq} in the thin-plate impact problem.

In summary, oriented dimensions of twenty-eight basic physical quantities are listed in Table 4. Compared with the traditional scalar dimensional analysis (such as MLT, VSG, VSM, DLV, et al.), the dimension of physical quantities is effectively extended. For example, the scalar dimension of stress, which is usually expressed as $L^{-1} M T^{-2}$, is extended to six different oriented dimensions in Table 4. The scalar dimension of strain, which is a naturally dimensionless quantity, is extended to different oriented dimensions in Table 4. Thus different forms of strain, plastic stain and equivalent strain are distinguished effectively. Since the direction of space is closely related to the dimensions of physical quantities, these newly-proposed oriented dimensions would lay the foundation for new similarity laws of geometric distortion later.

2.3. Dimensionless numbers

Referring to the previous DLV system [29], the density ρ , the three characteristic lengths L_x , L_y , L_z and the transverse velocity V_z are chosen as the bases of dimensional analysis. When using the Buckingham Π theorem [4,6] to respectively combine the five bases and every physical quantity in Table 4, twenty-three dimensionless numbers can be obtained as follows:

• six stress components

$$\begin{aligned}\Pi_{\sigma_x} &= \left[\frac{\rho V_z^2}{\sigma_x} \left(\frac{\bar{L}_x}{\bar{L}_z} \right)^2 \right], \Pi_{\sigma_y} = \left[\frac{\rho V_z^2}{\sigma_y} \left(\frac{\bar{L}_y}{\bar{L}_z} \right)^2 \right], \Pi_{\tau_{xy}} = \left[\frac{\rho V_z^2}{\tau_{xy}} \left(\frac{\sqrt{\bar{L}_x \bar{L}_y}}{\bar{L}_z} \right)^2 \right], \\ \Pi_{\sigma_z} &= \left[\frac{\rho V_z^2}{\sigma_z} \right], \Pi_{\tau_{xz}} = \left[\frac{\rho V_z^2}{\tau_{xz}} \left(\frac{\bar{L}_x}{\bar{L}_z} \right) \right], \Pi_{\tau_{yz}} = \left[\frac{\rho V_z^2}{\tau_{yz}} \left(\frac{\bar{L}_y}{\bar{L}_z} \right) \right];\end{aligned}\quad (5a-f)$$

- six strain components

$$\begin{aligned}\Pi_{\varepsilon_x} &= \left[\varepsilon_x \left(\frac{\bar{L}_x}{\bar{L}_z} \right)^2 \right], \Pi_{\varepsilon_y} = \left[\varepsilon_y \left(\frac{\bar{L}_y}{\bar{L}_z} \right)^2 \right], \Pi_{\gamma_{xy}} = \left[\gamma_{xy} \left(\frac{\sqrt{\bar{L}_x \bar{L}_y}}{\bar{L}_z} \right)^2 \right], \\ \Pi_{\varepsilon_z} &= [\varepsilon_z], \Pi_{\gamma_{xz}} = \left[\gamma_{xz} \left(\frac{\bar{L}_x}{\bar{L}_z} \right) \right], \Pi_{\gamma_{yz}} = \left[\gamma_{yz} \left(\frac{\bar{L}_y}{\bar{L}_z} \right) \right];\end{aligned}\quad (6a-f)$$

- three displacement components

$$\Pi_{\delta_x} = \left[\frac{\delta_x}{\bar{L}_x} \left(\frac{\bar{L}_x}{\bar{L}_z} \right)^2 \right], \Pi_{\delta_y} = \left[\frac{\delta_y}{\bar{L}_y} \left(\frac{\bar{L}_y}{\bar{L}_z} \right)^2 \right], \Pi_{\delta_z} = \left[\frac{\delta_z}{\bar{L}_z} \right];\quad (7a-c)$$

- time, impact mass and impulse pressure

$$\Pi_t = \left[\frac{tV_z}{\bar{L}_z} \right], \Pi_G = \left[\frac{G}{\rho(\bar{L}_x \bar{L}_y \bar{L}_z)} \right], \Pi_{P_z} = \left[\frac{P_z}{\rho V_z^2} \right];\quad (8a-c)$$

- equivalent stress and equivalent strain

$$\Pi_{\sigma_{eq}} = \left[\frac{\rho V_z^2}{\sigma_{eq}} \left(\frac{\bar{L}_{xy}}{\bar{L}_z} \right)^2 \right], \Pi_{\varepsilon_{eq}} = \left[\varepsilon_{eq} \left(\frac{\bar{L}_{xy}}{\bar{L}_z} \right)^2 \right];\quad (9a-b)$$

- three plastic modified train components

$$\Pi_{\varepsilon_z^{mod}} = \left[\varepsilon_z \left(\frac{\bar{L}_{xy}}{\bar{L}_z} \right)^2 \right], \Pi_{\gamma_{xz}^{mod}} = \left[\gamma_{xz} \left(\frac{\bar{L}_{xy}}{\bar{L}_z} \right)^3 \right], \Pi_{\gamma_{yz}^{mod}} = \left[\gamma_{yz} \left(\frac{\bar{L}_{xy}}{\bar{L}_z} \right)^3 \right];\quad (10a-c)$$

where $\sqrt{\bar{L}_x \bar{L}_y}$ in the numbers $\Pi_{\tau_{xy}}$ and $\Pi_{\gamma_{xy}}$ represents the characteristic length of the anisotropic x-y plane; while \bar{L}_{xy} in the numbers $\Pi_{\sigma_{eq}}$, $\Pi_{\varepsilon_{eq}}$, $\Pi_{\varepsilon_z^{mod}}$, $\Pi_{\gamma_{xz}^{mod}}$ and $\Pi_{\gamma_{yz}^{mod}}$ represents the characteristic lengths \bar{L}_x and \bar{L}_y of the isotropic x-y plane.

Recall that, in the previous DLV system, the stress σ , the strain ε , the displacement δ , the time t , the impact mass G and the impulse pressure P_z are dimensionless as $\left[\frac{\rho V^2}{\sigma} \right]$, $[\varepsilon]$, $\left[\frac{\delta}{\bar{L}} \right]$, $\left[\frac{tV}{\bar{L}} \right]$, $\left[\frac{G}{\rho \bar{L}^3} \right]$ and $\left[\frac{\rho V^2}{P_z} \right]$, respectively. In contrast, the dimensionless numbers in Eqs. (5)-(10) show more geometric and directional characteristics of space. The advantages of the above proposed dimensionless numbers are as follows.

- (1) These dimensionless numbers are all related to the spatial directional characteristic lengths. Meanwhile, simple power relationships, expressed as the powers $n = 0, 1, 2, 3$ of the ratios of the characteristic lengths (i.e., \bar{L}_x/\bar{L}_z , \bar{L}_y/\bar{L}_z , $\sqrt{\bar{L}_x \bar{L}_y}/\bar{L}_z$ and \bar{L}_{xy}/\bar{L}_z), are founded in the directional dimensionless numbers of Eqs. (5), (6), (7), (9) and (10).
- (2) The numbers $\Pi_{\sigma_x} - \Pi_{\tau_{yz}}$, $\Pi_{\varepsilon_x} - \Pi_{\gamma_{yz}}$ and $\Pi_{\delta_x} - \Pi_{\delta_z}$ can be expressed as the three tensor forms

$$\begin{aligned}\Pi_{\sigma_{ij}} &= \left[\frac{\rho V_z^2}{\sigma_{ij}} \left(\frac{\sqrt{\bar{L}_i \bar{L}_j}}{\bar{L}_z} \right)^2 \right], \Pi_{\varepsilon_{ij}} = \left[\varepsilon_{ij} \left(\frac{\sqrt{\bar{L}_i \bar{L}_j}}{\bar{L}_z} \right)^2 \right], \\ \Pi_{\delta_i} &= \left[\frac{\delta_i}{\bar{L}_i} \left(\frac{\sqrt{\bar{L}_i \bar{L}_j}}{\bar{L}_z} \right)^2 \right] \text{ (no sum on i,j)},\end{aligned}\quad (11a-c)$$

where $i, j = x, y, z$. And the numbers $\Pi_{\sigma_{ij}}$ and $\Pi_{\varepsilon_{ij}}$ can be suitable for representing similarity laws of the orthotropic elastic materials, which is presented in Appendix A.

- (1) The numbers $\Pi_{\sigma_{eq}}$ and $\Pi_{\varepsilon_{eq}}$ can be generalized to the forms $\Pi_{\sigma_{eq}}(n) = \left[\frac{\rho V_z^2}{\sigma_{eq}} \left(\frac{\bar{L}_{xy}}{\bar{L}_z} \right)^n \right]$ and $\Pi_{\varepsilon_{eq}}(n) = \left[\varepsilon_{eq} \left(\frac{\bar{L}_{xy}}{\bar{L}_z} \right)^n \right]$, respectively. In particular, $\Pi_{\sigma_{eq}}$ can be explained as the well-known Zhao's response number $R_n(n = 2) = \left[\frac{\rho V_0^2}{\sigma_0} \left(\frac{\bar{L}}{\bar{H}} \right)^2 \right]$. The different physical meaning of the exponent n can be understood by the response number and the damage number. For the thin-plate model with the isotropic x-y plane direction but anisotropic z direction, $n = 2$ and $\Pi_{\sigma_{eq}}(2)$ is equivalent to the Zhao's response number $R_n(n = 2) = \left[\frac{\rho V_0^2}{\sigma_0} \left(\frac{\bar{L}}{\bar{H}} \right)^2 \right]$. While, for structures with the isotropic three-dimensional space, $n = 0$ and $\Pi_{\sigma_{eq}}(0)$ is equivalent to $R_n(n = 0) = \left[\frac{\rho V_0^2}{\sigma_0} \right]$ (i.e., the Johnson's damage number D_n).
- (2) More interestingly, physical implications of these dimensionless numbers are very clear. For example, the number Π_{σ_x} represents the similarity of bending moment by the ratio of the inertia moment $\left[(\rho \bar{L}_x \bar{L}_y \bar{L}_z) \left(\frac{V_z^2}{\bar{L}_z} \right) \bar{L}_x \right]$ to the structural internal bending moment $[\sigma_x(\bar{L}_y \bar{L}_z)] \bar{L}_z$, where $\left(\frac{V_z^2}{\bar{L}_z} \right)$ represents the inertial acceleration along the z-axis; $[\sigma_x(\bar{L}_y \bar{L}_z)]$ represents the force along the x-axis. The number $\Pi_{\tau_{xy}}$ represents the ratio of the inertia torque along the x-axis, $\left[(\rho \bar{L}_x \bar{L}_y \bar{L}_z) \left(\frac{V_z^2}{\bar{L}_z} \right) \bar{L}_y \right]$, to the structural internal torque along the x-axis, $[\tau_{xy}(\bar{L}_y \bar{L}_z)] \bar{L}_z$. The number $\Pi_{\tau_{xz}}$ represents the similarity of force by the ratio of the inertia force $\left[(\rho \bar{L}_x \bar{L}_y \bar{L}_z) \left(\frac{V_z^2}{\bar{L}_z} \right) \bar{L}_z \right]$ to the structural internal shear forces $[\tau_{xz}(\bar{L}_y \bar{L}_z)]$. The numbers Π_{ε_x} represent the similarity of deformation by the ratio of the internal strain ε_x to the structural characteristic strain $(\bar{L}_z/\bar{L}_x)^2$ at the x-direction. The number Π_t represents the similarity of time by the ratio of the time t to the characteristic time (\bar{L}_z/V_z) . The number Π_G represents the similarity of inertia by the ratio of the impact mass G to the structural mass $(\rho \bar{L}_x \bar{L}_y \bar{L}_z)$.

Since these new proposed numbers are based on the oriented-density-length-velocity bases, they can be termed as the ODLV system.

2.4. Scaling factors

The well-known similarity theorem asserts that the dimensionless numbers between the scaled model and the prototype should be completely equal. In general, the equality relations are expressed as scaling factors of the physical quantities to conduct the forward scaling and the reverse prediction.

For example, when using the number Π_{σ_x} (Eq. (5a)), the equality $(\Pi_{\sigma_x})_m = (\Pi_{\sigma_x})_p$ leads to the scaling factor β_{σ_x} as

Table 5

Main scaling factors of structural impact in the ODLV.

Variable	Scaling factor	Variable	Scaling factor
Length \bar{L}_x	$\beta_{\bar{L}_x} = (\bar{L}_x)_m / (\bar{L}_x)_p$	Strain ϵ_z	$\beta_{\epsilon_z} = 1$
Length \bar{L}_y	$\beta_{\bar{L}_y} = (\bar{L}_y)_m / (\bar{L}_y)_p$	Strain γ_{xz}	$\beta_{\gamma_{xz}} = (\beta_{\bar{L}_x} / \beta_{\bar{L}_y})$
Length \bar{L}_z	$\beta_{\bar{L}_z} = (\bar{L}_z)_m / (\bar{L}_z)_p$	Strain γ_{yz}	$\beta_{\gamma_{yz}} = (\beta_{\bar{L}_x} / \beta_{\bar{L}_y})$
Density ρ	$\beta_\rho = \rho_m / \rho_p$	Time t	$\beta_t = (\beta_{\bar{L}_x} / \beta_{V_z})^2$
Velocity V_z	$\beta_{V_z} = (V_z)_m / (V_z)_p$	Displacement δ_x	$\beta_{\delta_x} = \beta_{\bar{L}_x} (\beta_{\bar{L}_x} / \beta_{\bar{L}_z})^2$
Stress σ_x	$\beta_{\sigma_x} = (\beta_\rho \beta_{V_z}^2) (\beta_{\bar{L}_x} / \beta_{\bar{L}_z})^2$	Displacement δ_y	$\beta_{\delta_y} = \beta_{\bar{L}_y} (\beta_{\bar{L}_x} / \beta_{\bar{L}_y})^2$
Stress σ_y	$\beta_{\sigma_y} = (\beta_\rho \beta_{V_z}^2) (\beta_{\bar{L}_y} / \beta_{\bar{L}_z})^2$	Displacement δ_z	$\beta_{\delta_z} = \beta_{\bar{L}_z}$
Stress σ_z	$\beta_{\sigma_z} = (\beta_\rho \beta_{V_z}^2)$	Impact mass G	$\beta_G = \beta_\rho (\beta_{\bar{L}_x} \beta_{\bar{L}_y} \beta_{\bar{L}_z})$
Stress τ_{xy}	$\beta_{\tau_{xy}} = (\beta_\rho \beta_{V_z}^2) (\sqrt{\beta_{\bar{L}_x} \beta_{\bar{L}_y}} / \beta_{\bar{L}_z})^2$	Surface pressure P_z	$\beta_{P_z} = (\beta_\rho \beta_{V_z}^2)$
Stress τ_{xz}	$\beta_{\tau_{xz}} = (\beta_\rho \beta_{V_z}^2) (\beta_{\bar{L}_x} / \beta_{\bar{L}_z})$	Equivalent stress σ_{eq}	$\beta_{\sigma_{eq}} = (\beta_\rho \beta_{V_z}^2) (\beta_{\bar{L}_x} / \beta_{\bar{L}_z})^2$
Stress τ_{yz}	$\beta_{\tau_{yz}} = (\beta_\rho \beta_{V_z}^2) (\beta_{\bar{L}_y} / \beta_{\bar{L}_z})$	Equivalent strain ϵ_{eq}	$\beta_{\epsilon_{eq}} = (\beta_{\bar{L}_x} / \beta_{\bar{L}_y})^2$
Strain ϵ_x	$\beta_{\epsilon_x} = (\beta_{\bar{L}_x} / \beta_{\bar{L}_z})^2$	Plastic strain ϵ_z	$\beta_{\epsilon_z}^{mod} = (\beta_{\bar{L}_x} / \beta_{\bar{L}_y})^2$
Strain ϵ_y	$\beta_{\epsilon_y} = (\beta_{\bar{L}_y} / \beta_{\bar{L}_z})^2$	Plastic strain γ_{xz}	$\beta_{\gamma_{xz}}^{mod} = (\beta_{\bar{L}_x} / \beta_{\bar{L}_y})^3$
Strain γ_{xy}	$\beta_{\gamma_{xy}} = (\beta_{\bar{L}_x} / \sqrt{\beta_{\bar{L}_x} \beta_{\bar{L}_y}})^2$	Plastic strain γ_{yz}	$\beta_{\gamma_{yz}}^{mod} = (\beta_{\bar{L}_y} / \beta_{\bar{L}_z})^3$

$$\frac{\rho_m (V_z)_m^2}{(\sigma_x)_m} \left[\frac{(\bar{L}_x)_m}{(\bar{L}_z)_m} \right]^2 = \frac{\rho_p (V_z)_p^2}{(\sigma_x)_p} \left[\frac{(\bar{L}_x)_p}{(\bar{L}_z)_p} \right]^2 \rightarrow \beta_{\sigma_x} = \beta_\rho \beta_{V_z} (\beta_{\bar{L}_x} / \beta_{\bar{L}_z})^2. \quad (12)$$

Similarly, other scaling factors can be obtained by the equality of the numbers $\Pi_{\sigma_y} - \Pi_{\gamma_{yz}}^{mod}$ (Eqs. (5b)-(10c)). Main scaling factors of the ODLV are listed in Table 5.

It can be seen that these factors are directly expressed in terms of the five basic scaling factors β_ρ , $\beta_{\bar{L}_x}$, $\beta_{\bar{L}_y}$, $\beta_{\bar{L}_z}$ and β_{V_z} ($\beta_{\bar{L}_{xy}} = \beta_{\bar{L}_x} = \beta_{\bar{L}_y}$ for the isotropic rigid-plastic materials). Comparing with the previous scaling relations (see Tables 1, 2 and 3), it can be found that the basic geometric scaling factor of the structure expands from a single scalar factor β to the three directional factors $\beta_{\bar{L}_x}$, $\beta_{\bar{L}_y}$ and $\beta_{\bar{L}_z}$. In addition, the strain scaling is closely related to the scaling of geometric characteristic lengths in different directions, which breaks the invariance of strain in previous scaling relations.

2.5. Scaling procedure

Using the factors in Table 5 to carry out scaling procedure, the distortion problems could be further taken into account.

- The geometric distortion is defined as $\beta_{\bar{L}_z} \neq \beta_{\bar{L}_{xy}}$;
- The material distortion should respect the constitutive equation with strain hardening and strain rate effects, $\sigma_{eq} = f(\epsilon_{eq}, \dot{\epsilon}_{eq})$, where f is a function representing stress in terms of strain and strain rate.
- Other distortion, for example, the gravity distortion should respect an additional constraint $\beta_{V_z} = \sqrt{\beta_{\bar{L}_z}}$ about the transverse gravity acceleration g_z . The constraint is obtained from the dimensionless number of gravity, $\Pi_{g_z} = \frac{g_z \bar{L}_z}{V_z^2}$, and its scaling factor $\beta_{V_z} = \sqrt{\beta_{g_z} \beta_{\bar{L}_z}} = \sqrt{\beta_{\bar{L}_z}}$ ($\beta_{g_z} = 1$ usually for earth surface locations).

2.5.1. Geometric and material distortion

For the constitutive equation of the scaled model and the prototype, the consistency relation $f_m((\epsilon_{eq})_m, (\dot{\epsilon}_{eq})_m) / \beta_{\sigma_{eq}} = f_p((\epsilon_{eq})_p, (\dot{\epsilon}_{eq})_p)$ should be satisfied in the similarity laws. Substituting the scaling factors of $\beta_{\sigma_{eq}}$, $\beta_{\epsilon_{eq}}$ and $\beta_{\dot{\epsilon}_{eq}} = \beta_{\epsilon_{eq}} / \beta_t$ (see Table 5) into that relation, a key constraint

among the basic scaling factors β_ρ , $\beta_{\bar{L}_{xy}}$, $\beta_{\bar{L}_z}$ and β_{V_z} is obtained as

$$f_m \left\{ (\epsilon_{eq})_p \left(\frac{\beta_{\bar{L}_x}}{\beta_{\bar{L}_{xy}}} \right)^2, (\dot{\epsilon}_{eq})_p \frac{\beta_{V_z}}{\beta_{\bar{L}_z}} \left(\frac{\beta_{\bar{L}_z}}{\beta_{\bar{L}_{xy}}} \right)^2 \right\} \frac{1}{\beta_\rho \beta_{V_z}^2} \left(\frac{\beta_{\bar{L}_z}}{\beta_{\bar{L}_{xy}}} \right)^2 = f_p \left\{ (\epsilon_{eq})_p, (\dot{\epsilon}_{eq})_p \right\}. \quad (13)$$

Equation (13) indicates the correlation between the basic scaling factor and the constitutive equation. If the geometrical and material properties of the structure are specified at a scaling, $\beta_{\bar{L}_{xy}}$, $\beta_{\bar{L}_z}$ and β_ρ are known whether for the geometrically similar scaling $\beta_{\bar{L}_z} = \beta_{\bar{L}_{xy}}$ or the geometrically distorted scaling $\beta_{\bar{L}_z} \neq \beta_{\bar{L}_{xy}}$. The dynamic responses $(\epsilon_{eq})_p$ and $(\dot{\epsilon}_{eq})_p$ can be approximately replaced by the average strain and average strain rate of the structure, respectively. Although this equivalent method usually results in incomplete similarity due to the material constitutive equations employed, it is proved to be feasible by previous works [14,15,18,21]. In addition, $\beta_{\bar{L}_{xy}}$ needs to be specified in advance to provide a basic reference for scaling of other variables. Then, three initial variables, β_ρ , $\beta_{\bar{L}_z}$ and β_{V_z} , can be solved from Eq. (13) to conduct scaling procedure, as follows.

- Impact velocity correction.

If the density and geometrical thickness are not corrected, the impact velocity of scaled model can be independently corrected as $(V_z)_m = (V_z)_p \beta_{V_z}$ by the correction factor

$$\beta_{V_z} = \left(\frac{\beta_{\bar{L}_z}}{\beta_{\bar{L}_{xy}}} \right) \sqrt{\frac{f_m \left\{ (\epsilon_{eq})_p \left(\frac{\beta_{\bar{L}_x}}{\beta_{\bar{L}_{xy}}} \right)^2, (\dot{\epsilon}_{eq})_p \frac{\beta_{V_z}}{\beta_{\bar{L}_z}} \left(\frac{\beta_{\bar{L}_z}}{\beta_{\bar{L}_{xy}}} \right)^2 \right\}}{f_p \left\{ (\epsilon_{eq})_p, (\dot{\epsilon}_{eq})_p \right\}}} \frac{1}{\beta_\rho}. \quad (14)$$

The solution to β_{V_z} can be obtained by a numerical method of iteration [41] since $f_m \{\dots\}$ also contains β_{V_z} .

- Density correction.

If the impact velocity and geometrical thickness are not corrected, the density of scaled model can be independently corrected as $\rho_m = \rho_p \beta_\rho$ by the correction factor $\beta_\rho = \frac{f_m \{\dots\}}{f_p \{\dots\}} \frac{1}{\beta_{V_z}^2} \left(\frac{\beta_{\bar{L}_z}}{\beta_{\bar{L}_{xy}}} \right)^2$, where the omitted contents of curly bracket in $f_m \{\dots\}$ and $f_p \{\dots\}$ are identical with Eq. (13). The solution to β_ρ can be obtained directly without iteration since $f_m \{\dots\}$ does not contain β_ρ .

In a real experiment, the correction for structural density can be obtained indirectly by an additional mass technique. The technique, proposed by Jiang et al. [21], usually changes the density of the structure by evenly or discretely distributing the additional mass $\Delta M = M_p (\beta_\rho \beta_{\bar{L}_x} \beta_{\bar{L}_y} \beta_{\bar{L}_z} - 1)$ into each component of the scaled model. While, the correction for impact mass density can be obtained directly by correcting the mass, i.e. $G_m = G_p \beta_\rho (\beta_{\bar{L}_x} \beta_{\bar{L}_y} \beta_{\bar{L}_z})$.

- Geometrical thickness correction.

If the impact velocity and the density are not corrected, the thickness of scaled model can be independently corrected as $(L_z)_m = (L_z)_p \beta_{\bar{L}_z}$ by the correction factor $\beta_{\bar{L}_z} = \beta_{\bar{L}_{xy}} \beta_{V_z} \sqrt{\frac{f_p \{\dots\}}{f_m \{\dots\}} \beta_\rho}$, where the omitted contents of curly bracket in $f_m \{\dots\}$ and $f_p \{\dots\}$ are identical with Eq. (13). The solution to $\beta_{\bar{L}_z}$ needs iteration [41] since $f_m \{\dots\}$ also contain $\beta_{\bar{L}_z}$.

Recall that, in the previous works, correction of the impact velocity and the density are usually used to compensate for the material distortions. In here, a more comprehensive method is developed by further considering the geometric distortion in the two correction methods. In

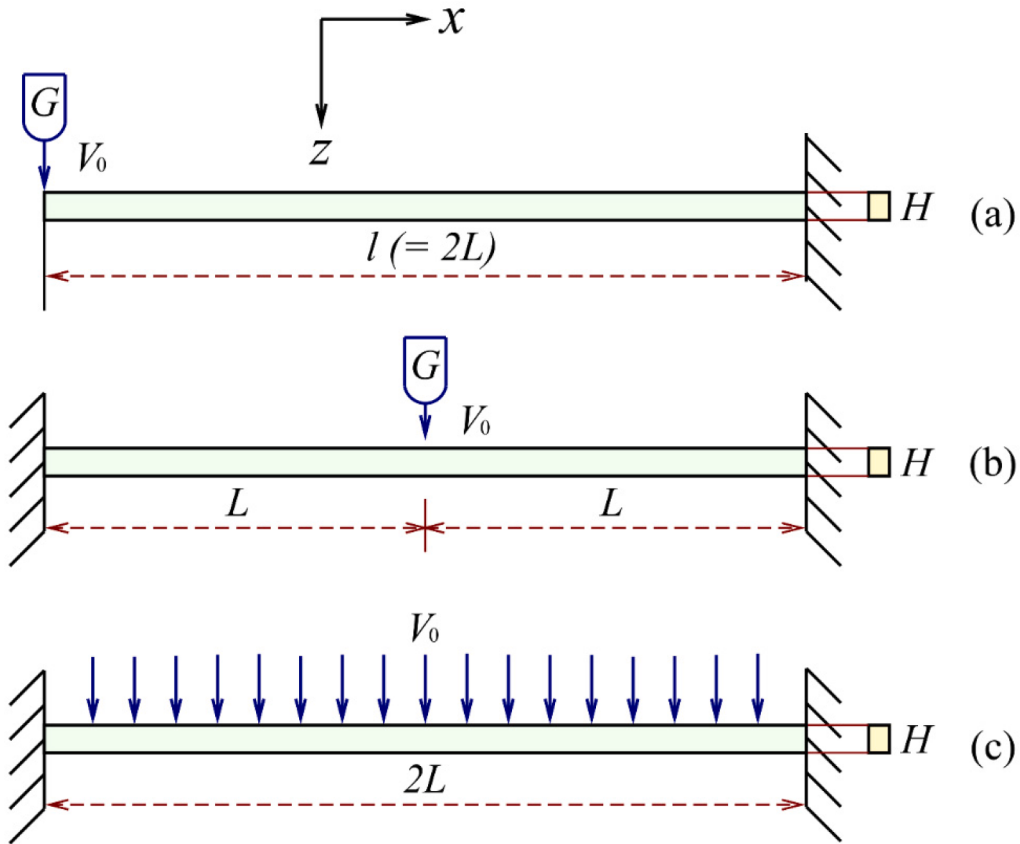


Fig. 2. Impacted beams. (a) A cantilever beam subjected to mass impact at the free end; (b) a clamped beam subjected to impact mass at mid span; (c) a clamped beam subjected to impulsive velocity on entire span.

addition, another important different aspect is that the strain and strain rate scaling is related to geometric distortion in Eq. (13), i.e. $\beta_{eq} \neq 1$ and $\beta_{eq} \neq (\beta_{V_z} / \beta_{L_z})$ for $\beta_{L_z} \neq \beta_{L_{xy}}$. When the strain fields need to be changed for distortion problems, the correction of geometrical thickness will have a unique advantage.

2.5.2. Other distortion

In addition to the three independent correcting methods, their combination provides a more powerful correction. When the combination correction methods are used to the geometric and material distortion, there are $(C_3^2 + C_3^3) = 4$ combining forms to make the factors β_{V_z} , β_ρ and β_{L_z} satisfy Eq. (13). More importantly, the combination correction can be used to address more distortion problems. For example, for the gravity distortion, with the combination of Eq. (13) and the additional constraint $\beta_{V_z} = \sqrt{\beta_{L_z}}$, the combined correction procedures are obtained as follows.

- The impact velocity and the density can be corrected in combination when the factors β_{V_z} and β_ρ satisfy the equation group $\beta_{V_z} = \sqrt{\beta_{L_z}}$ and Eq. (13) for the geometrically similar scaling $\beta_{L_z} = \beta_{L_{xy}}$ or the geometrically distorted scaling $\beta_{L_z} \neq \beta_{L_{xy}}$. The combination correction has been verified by the single-layer reticulated shells with the geometrically similar scaling in Ref. [21].
- The impact velocity (or density) and the geometrical thickness can be corrected in combination when the correcting factors β_{V_z} (or β_ρ) and β_{L_z} satisfy the equation group $\beta_{V_z} = \sqrt{\beta_{L_z}}$ and Eq. (13). The correction of velocity and thickness could be easier than the correction of density and velocity in the tests of simple beams and plates.

The above analysis lays the foundation for addressing various distortion problems in which three basic correction methods can be used in separation or in combination.

3. Analytical verification

In this section, the analytical models of beams are used to verify dimensionless numbers and scaling ability of the proposed similarity laws.

3.1. The beams subjected to impact mass and impulsive velocity

The impact models of rigid-plastic beams subjected to impact mass and impulsive velocity are shown in Fig. 2. Various response equations of these impacted beams are listed in Appendix B.

3.1.1. Dimensionless expression for response equations

When the structural geometric characteristics are considered by the different directional characteristic lengths L and H , dimensionless expression of the response equations should satisfy the directional homogeneity. For example, W_f and H have identical direction and should be combined to a dimensionless number W_f/H .

- For the cantilever beam subjected to impact mass, Eqs. (B.1a)-(B.1c) can be respectively re-expressed as the following forms with directional homogeneity

$$\left. \begin{aligned} \frac{W_f}{H} &= \frac{16}{3} \frac{\rho V_0^2}{\sigma_d} \left(\frac{L}{H} \right)^2 \kappa^2 \left[\frac{1}{1+2\kappa} + 2\ln \left(1 + \frac{1}{2\kappa} \right) \right] \\ \alpha_f \left(\frac{H}{L} \right) &= \frac{16}{3} \frac{\rho V_0^2}{\sigma_d} \left(\frac{L}{H} \right)^2 (1+3\kappa) \left(1 + \frac{1}{2\kappa} \right)^{-2} \\ \frac{T_f V_0}{H} &= 16 \frac{\rho V_0^2}{\sigma_d} \left(\frac{L}{H} \right)^2 \kappa \end{aligned} \right\}, \quad (15a-c)$$

- Similarly, for the clamped beam subjected to impact mass, Eqs. (B.2a) and (B.2b) (neglect shear strain) can be respectively re-expressed as

$$\left. \begin{aligned} \frac{W_f}{H} &= \frac{1}{2} \left[\left(1 + 4 \frac{\rho V_0^2}{\sigma_d} \left(\frac{L}{H} \right)^2 \kappa \right)^{1/2} - 1 \right] \\ \varepsilon_{eq} \left(\frac{L}{H} \right)^2 &= \begin{cases} \frac{3}{2} \left[\left(1 + 4 \frac{\rho V_0^2}{\sigma_d} \left(\frac{L}{H} \right)^2 \kappa \right)^{1/2} - 1 \right], & \text{for } \frac{W_f}{H} \leq 1 \\ \frac{1}{8} \left[\left(1 + 4 \frac{\rho V_0^2}{\sigma_d} \left(\frac{L}{H} \right)^2 \kappa \right)^{1/2} - 1 \right]^2 + \frac{5}{2}, & \text{for } \frac{W_f}{H} > 1 \end{cases} \end{aligned} \right\}. \quad (16a-b)$$

- For the clamped beam subjected to impulsive velocity, Eqs. (B.3a) and (B.3b) can be respectively re-expressed as

$$\left. \begin{aligned} \frac{W_f}{H} &= \frac{1}{2} \left[\left(1 + 3 \frac{\rho V_0^2}{\sigma_d} \left(\frac{L}{H} \right)^2 \right)^{1/2} - 1 \right] \\ \frac{\dot{\varepsilon}_{eq} H}{V_0} \left(\frac{L}{H} \right)^2 &= \frac{1}{3\sqrt{2}} \frac{W_f}{H} = \frac{1}{6\sqrt{2}} \left[\left(1 + 3 \frac{\rho V_0^2}{\sigma_d} \left(\frac{L}{H} \right)^2 \right)^{1/2} - 1 \right] \end{aligned} \right\}. \quad (17a-b)$$

Equations (15)-(17) show that, for these impacted beams, the seven response equations Eq. (B.1a)-Eq. (B.3b) can be reduced to the seven corresponding dimensionless functional relations. In these functional relations, the numbers $\left[\frac{\rho V_0^2}{\sigma_d} \left(\frac{L}{H} \right)^2 \right]$ and $\kappa = \left[\frac{G}{2\rho LBH} \right]$ (only appearing in the case of impact mass load) are two independent dimensionless input variables, while the numbers $\left[\frac{W_f}{H} \right]$, $\left[\alpha_f \left(\frac{H}{L} \right) \right]$, $\left[\frac{T_f V_0}{H} \right]$, $\left[\varepsilon_{eq} \left(\frac{L}{H} \right)^2 \right]$ and $\left[\frac{\dot{\varepsilon}_{eq} H}{V_0} \left(\frac{L}{H} \right)^2 \right]$ are respectively five independent dimensionless output variables.

In addition, two important points can be found: (1) the two independent dimensionless input variables are respectively in full accord with the numbers $\Pi_{\sigma_{eq}}$, $\Pi_{\alpha_{xz}} = \frac{\Pi_{\delta_x}}{\Pi_{\delta_x}} = \left[\frac{\delta_z}{\delta_x} \left(\frac{\bar{L}_x}{L_x} \right) \right] = \left[\alpha_{xz} \left(\frac{\bar{L}_x}{L_x} \right) \right]$, Π_t , $\Pi_{\varepsilon_{eq}}$ and $\Pi_{\dot{\varepsilon}_{eq}} = \frac{\Pi_{\dot{\varepsilon}_{eq}}}{\Pi_t} = \frac{\dot{\varepsilon}_{eq} \bar{L}_x}{V_z} \left(\frac{\bar{L}_{xy}}{L_z} \right)^2$ in the ODLV; (2) the expressions with the ODLV are more concise and clear than those with the DLV. For example, in the DLV, the dimensionless expression for Eq. (B.3a) usually uses the three numbers $\left[\frac{W_f}{L} \right]$, $\left[\frac{L}{H} \right]$ and $\left[\frac{\rho V_0^2}{\sigma_d} \right]$ [29]. While, Eq. (17a) uses the only two numbers $\left[\frac{W_f}{H} \right]$ and $\left[\frac{\rho V_0^2}{\sigma_d} \left(\frac{L}{H} \right)^2 \right]$ in the ODLV.

For the dimensionless expression ability used the ODLV, further

verification for high-dimensional structures of the plates can be found in Appendix C. In addition, it is also significant to find that, for more impact models of beams, square and rectangular plates, circular plates and circular membranes, the dimensionless response equation of final deflection is expressed by the similar forms with Eqs. (15a), (16a) and (17a) in the previous works [32] and [36]. In this paper, the dimensionless number of ODLV is used to conduct a more thorough and comprehensive analysis.

3.1.2. Scaling analysis

For the geometrically similar scaling $\beta_H = \beta_L$ or the geometrically-distorted scaling $\beta_H \neq \beta_L$, the similarity of Eqs. (15)-(17) requires the input variables L , H , ρ , σ_d , V_0 and G should respect $\left[\frac{\rho V_0^2}{\sigma_d} \left(\frac{L}{H} \right)^2 \right]_m = \left[\frac{\rho V_0^2}{\sigma_d} \left(\frac{L}{H} \right)^2 \right]_p$ and $\left[\frac{G}{2\rho LBH} \right]_m = \left[\frac{G}{2\rho LBH} \right]_p$, which are equivalent to the two input relations $\beta_{\sigma_d} = (\beta_\rho \beta_{V_0}^2)(\beta_L / \beta_H)^2$ and $\beta_G = \beta_\rho (\beta_L \beta_B \beta_H)$, respectively.

The output variables W_f , α_f , T_f , ε_{eq} and $\dot{\varepsilon}_{eq}$ should respect $\left[\frac{W_f}{H} \right]_m = \left[\frac{W_f}{H} \right]_p$, $\left[\alpha_f \left(\frac{H}{L} \right) \right]_m = \left[\alpha_f \left(\frac{H}{L} \right) \right]_p$, $\left[\frac{T_f V_0}{H} \right]_m = \left[\frac{T_f V_0}{H} \right]_p$, $\left[\varepsilon_{eq} \left(\frac{L}{H} \right)^2 \right]_m = \left[\varepsilon_{eq} \left(\frac{L}{H} \right)^2 \right]_p$ and $\left[\frac{\dot{\varepsilon}_{eq} H}{V_0} \left(\frac{L}{H} \right)^2 \right]_m = \left[\frac{\dot{\varepsilon}_{eq} H}{V_0} \left(\frac{L}{H} \right)^2 \right]_p$, which are equivalent to the five output relations $\beta_{W_f} = \beta_H$, $\beta_{\alpha_f} = (\beta_L / \beta_H)$, $\beta_{T_f} = \beta_H / \beta_{V_0}$, $\beta_{\varepsilon_{eq}} = (\beta_H / \beta_L)^2$ and $\beta_{\dot{\varepsilon}_{eq}} = (\beta_{V_0} / \beta_H)(\beta_H / \beta_L)^2$, respectively.

In what follows, the scaling procedures could be implemented as follows:

- Independent correction: (1) impact velocity correction, if the input variables satisfy $\beta_L = L_m / L_p$, $\beta_H = H_m / H_p$, $\beta_\rho = \rho_m / \rho_p$, $\beta_G = \beta_\rho (\beta_L \beta_B \beta_H)$ and the correction factor $\beta_{V_0} = (\beta_H / \beta_L) \sqrt{\beta_{\sigma_d} / \beta_\rho}$, the output variables will accurately satisfy the above five output relations; (2) density correction, if the input variables satisfy $\beta_L = L_m / L_p$, $\beta_H = H_m / H_p$, $\beta_{V_0} = 1$ and the correction factors $\beta_\rho = (\beta_H / \beta_L)^2 (\beta_{\sigma_d} / \beta_{V_0}^2)$ and $\beta_G = \beta_\rho (\beta_L \beta_B \beta_H)$, the output variables will accurately satisfy the above five output relations; (3) geometrical thickness correction, if the input variables satisfy $\beta_L = L_m / L_p$, $\beta_{V_0} = 1$, $\beta_\rho = \rho_m / \rho_p$ and the correction factors $\beta_H = \beta_L \beta_{V_0} \sqrt{\beta_\rho / \beta_{\sigma_d}}$ and $\beta_G = \beta_\rho (\beta_L \beta_B \beta_H)$, the output variables will accurately satisfy the above five output relations.
- Combination correction of β_{V_0} , β_ρ and β_H : besides the above three independent correction cases, if the input variables of impact velocity, density and geometrical thickness are corrected to satisfy the relation $\beta_{\sigma_d} = (\beta_\rho \beta_{V_0}^2)(\beta_L / \beta_H)^2$, and the impact mass satisfy $\beta_G = \beta_\rho (\beta_L \beta_B \beta_H)$, the above five output relations will also be accurately satisfied.

The above scaling procedures verify the proposed correction methods in Section 2.5 to compensate for the distortions of geometry and materials.

4. Numerical analysis

In this section, a numerical model of impacted circular plate is used to validate more details of the proposed similarity laws from the viewpoints of both spatial and temporal fields.

4.1. A clamped circular plate subjected to dynamic pressure pulse

The model of a clamped circular plate subjected to two different

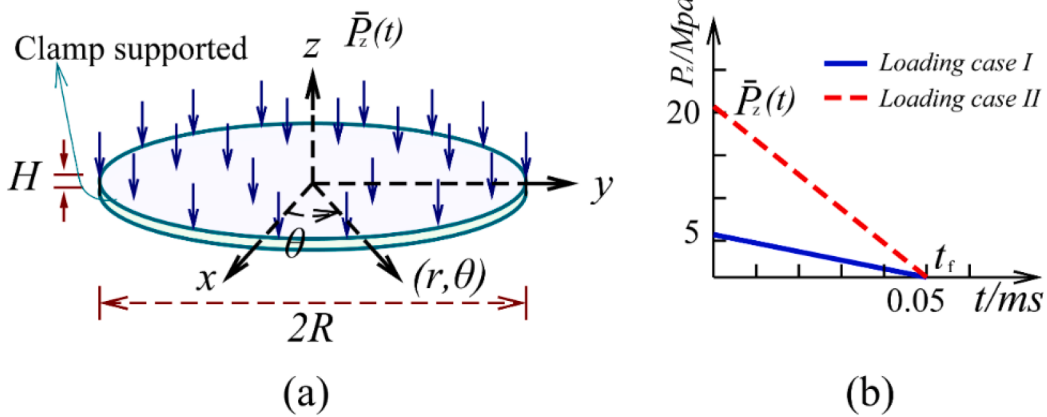


Fig. 3. A clamped circular plate with $R = 125 \text{ mm}$ and $H = 2 \text{ mm}$ is subjected to pressure pulse loading. (a) Impacted circular plate. (b) loading cases.

Table 6
Scaling factors of input parameters for circular plates.

Factor	Prototype	Model $\eta = 1.5$	Model $\eta = 2.0$	Model $\eta = 3.0$	Model $\eta = 4.0$
β_r	1	0.1	0.1	0.1	0.1
β_θ	1	1	1	1	1
β_H	1	0.15	0.2	0.3	0.4
β_p	1	1	1	1	1
β_{V_z}	1	1.5	2	3	4
β_t	1	0.1	0.1	0.1	0.1
β_{P_z}	1	2.25	4	9	16

degrees of pressure pulse loading in the cylindrical coordinate system (r, θ, z) , is shown in Fig. 3. The two loading cases are approximately equivalent to impulsive velocity of $V_0 = 8 \text{ m/s}$ and 32 m/s according to the momentum theorem (i.e., $(P_z \pi R^2) t_f / 2 = (\rho \pi R^2 H) V_0$).

From the cartesian coordinate system (x, y, z) in Section 2 to the present cylindrical coordinate system (r, θ, z) , the oriented dimensional analysis can be easily obtained by the corresponding relations

$$\text{Length dimension : } \mathbb{L}_x \rightarrow \mathbb{L}_r = \mathbb{R}_r, \quad \mathbb{L}_y \rightarrow \mathbb{L}_\theta = \mathbb{R}_r \mathbb{A}_\theta, \quad \mathbb{L}_z \rightarrow \mathbb{L}_z \}, \\ \text{Characteristic length : } \overline{\mathbb{L}}_x \rightarrow \overline{\mathbb{L}}_r = \overline{R}, \quad \overline{\mathbb{L}}_y \rightarrow \overline{\mathbb{L}}_\theta = \overline{R} \overline{\theta}, \quad \overline{\mathbb{L}}_z \rightarrow \overline{\mathbb{L}}_z \}, \quad (18)$$

where \mathbb{R} and \mathbb{A} represent the dimensions of radius and angle, respectively; \overline{R} and $\overline{\theta}$ represent characteristic radius and characteristic angle, respectively; $\mathbb{L}_r = \mathbb{R}_r$, $\mathbb{L}_\theta = \mathbb{R}_r \mathbb{A}_\theta$ and \mathbb{L}_z are three oriented length dimensions; $\overline{\mathbb{L}}_r = \overline{R}$, $\overline{\mathbb{L}}_\theta = \overline{R} \overline{\theta}$ and $\overline{\mathbb{L}}_z$ are three directional characteristic lengths. For this axisymmetric impacted model, the characteristic angle $\overline{\theta} = 2\pi$ is a constant and therefore is meaningless in dimensional analysis. The corresponding dimensionless numbers in the cartesian coordinate system from Eqs. (5)-(10) can be seen in the later analysis.

4.1.1. Numerical modeling

The finite element model of a circular plate is established in the ABAQUS software. The CAX4R axisymmetric elements are adopted to discretize structure with 450 elements in radius and 8 elements in thickness. The plate is fully clamped along its external boundary. Four numerical models with $R = 12.5 \text{ mm}$ and $H = 0.3, 0.4, 0.6, 0.8 \text{ mm}$ are established to represent four scaled models of geometric distortion, respectively. The distortion degrees are respectively represented by $\eta = \beta_H / \beta_R = 1.5, 2, 3, 4$, and the thicknesses are discretized with $8\eta = 12, 16, 24, 32$ elements, respectively. For prototype and scaled models, the

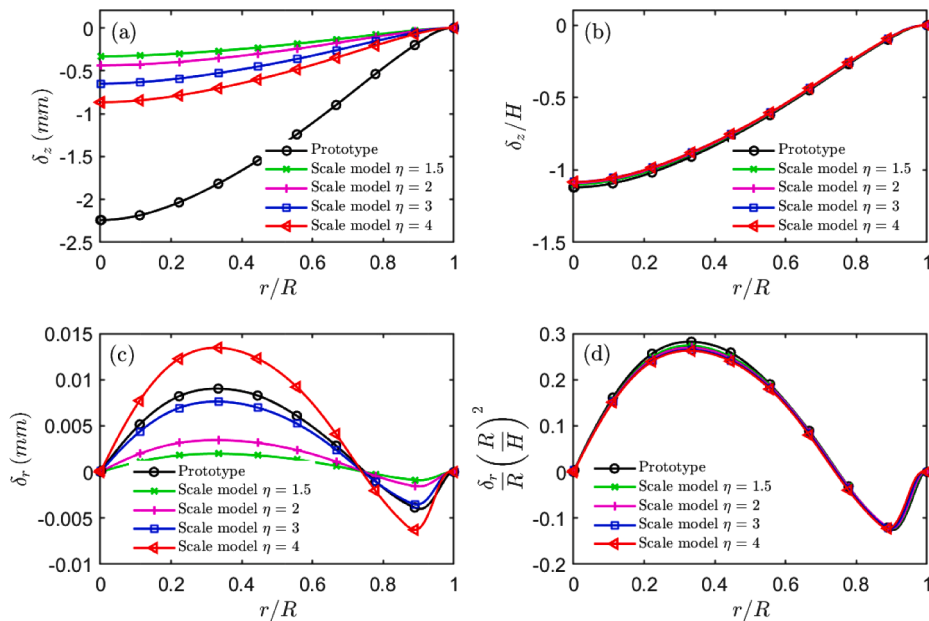


Fig. 4. The similarity of displacement components on the neutral plane for circular plates at final time $tV_0/H = 1.344$ (Loading case I).

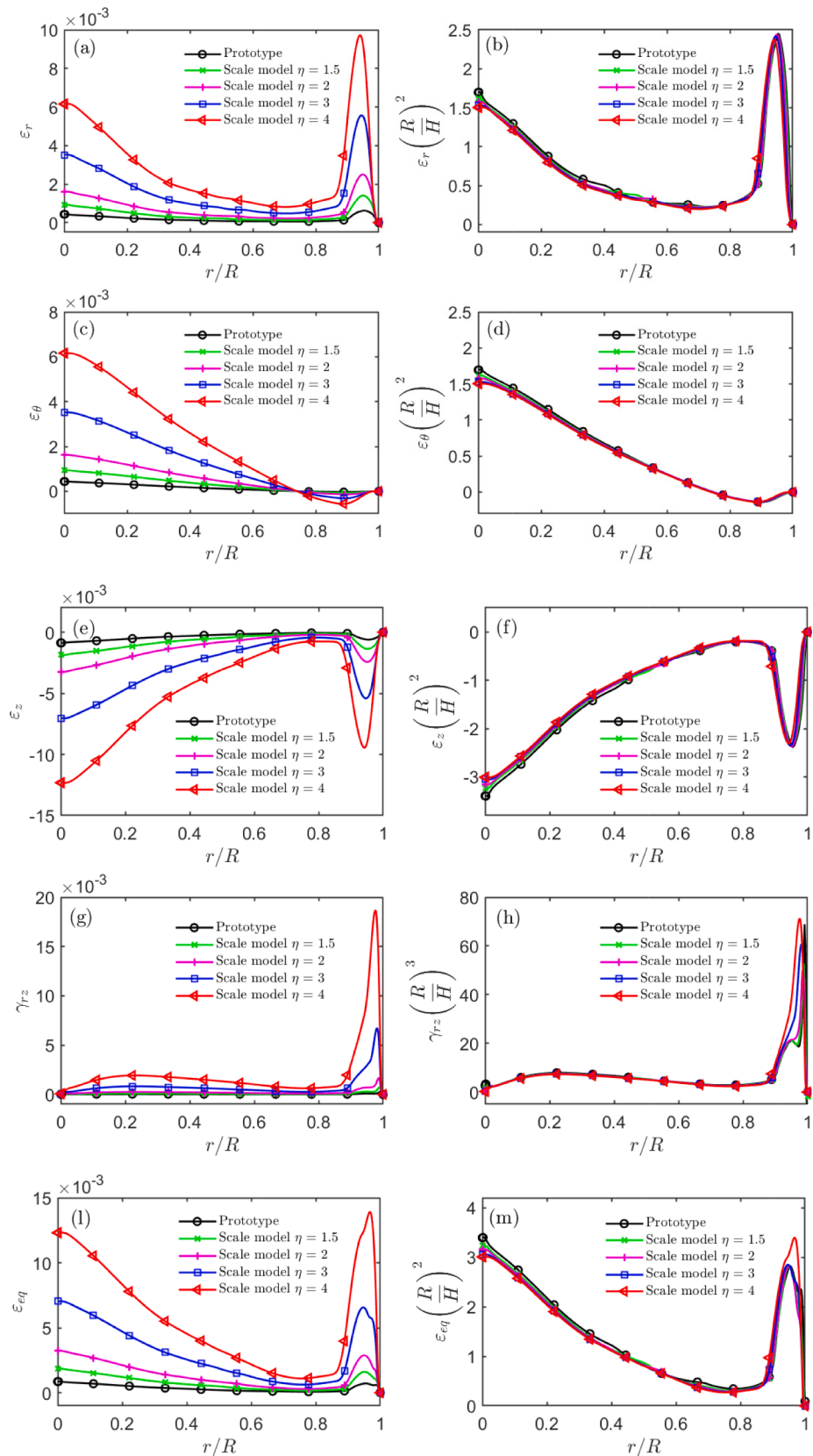


Fig. 5. The similarity of strain on the neutral plane for circular plates at final time $tV_0/H = 1.344$ (Loading case I).

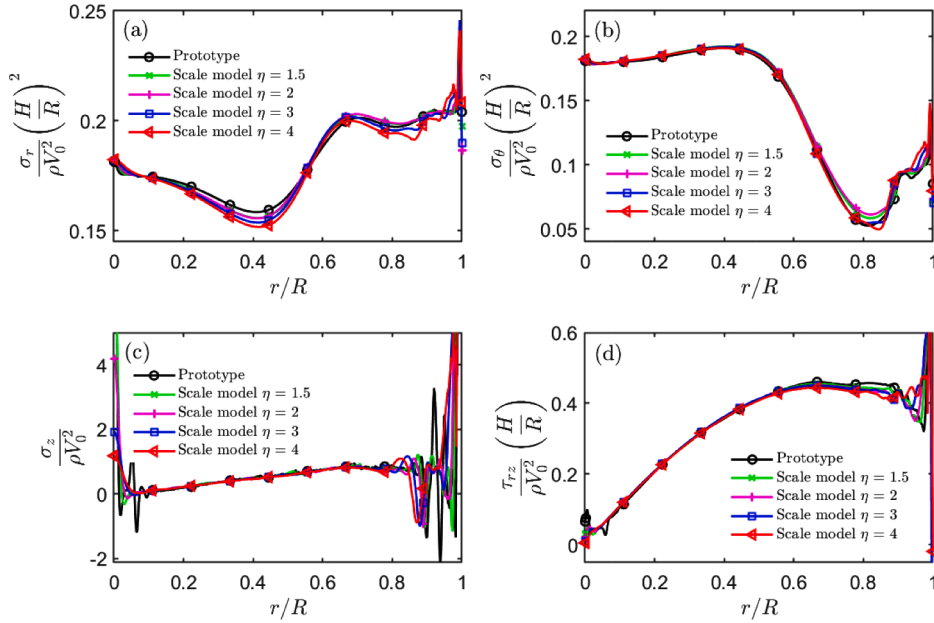


Fig. 6. The similarity of stress components on the neutral plane for circular plates at the time $tV_0/H = 1.2$ (Loading case I).

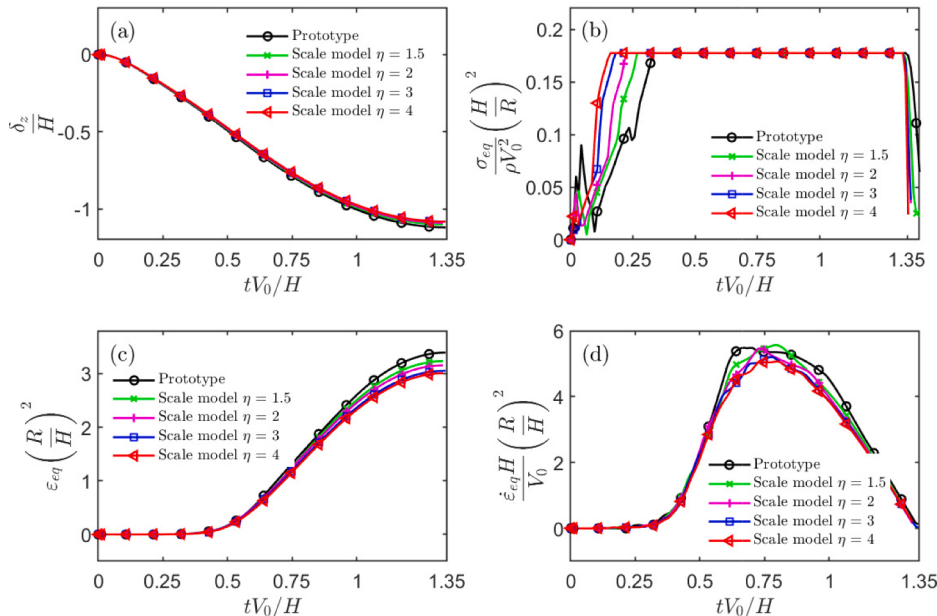


Fig. 7. Similarity of center point during deformation history for circular plates (Loading case I).

rigid-perfectly plastic material model with $\sigma_d = 350 \text{ MPa}$ (referring to 1006 Steel [42]) is adopted to simplify the constitutive equation. Since ignoring the material strain hardening and strain rate effects, Eq. (13) can be exactly established for any dynamic response $(\varepsilon_{eq})_p$ and $(\dot{\varepsilon}_{eq})_p$. To intuitively show the similarity of geometric distortion with more complex constitutive models, a numerical verification used Johnson-Cook constitutive model [42] is presented in Appendix D. The elastic modulus is set 1000 times larger than the actual value of $E = 200 \text{ GPa}$ to eliminate the similarity errors caused by elasticity as much as possible (the technique is verified by Ref. [17]). The material density is $7.89 \times 10^3 \text{ kg/m}^3$ and Poisson ratio is 0.3. The velocity factor is obtained according to $\beta_{V_z} = (\rho_H/\rho_R)\sqrt{\rho_{\sigma_0}/\rho_p}$ (Eq. (14)). The amplitude and loading time of dynamic pressure pulse are scaled from the prototype by $\beta_z = \rho_p \beta_{V_z}^2$ and $\beta_t = \beta_{L_z}/\beta_{V_z}$ (Table 5), respectively. Other input conditions are

completely identical with the prototype. Scaling factors of the input parameters are listed in Table 6.

4.1.2. Results analysis

- Loading Case I
 - (1) Displacement

For this axisymmetric problem, the similarity of displacement in the spatial fields is evaluated by the displacement components δ_z and δ_r , with the results plotted in Fig. 4. The two displacement components between the prototype and the scaled models show significant difference along dimensionless spatial positions of $\Pi_r = \frac{r}{R}$, as shown in Fig. 4a and c. According to the arctangent of $(\delta_z)_{max}/R$ in Fig. 4a, the rotations of

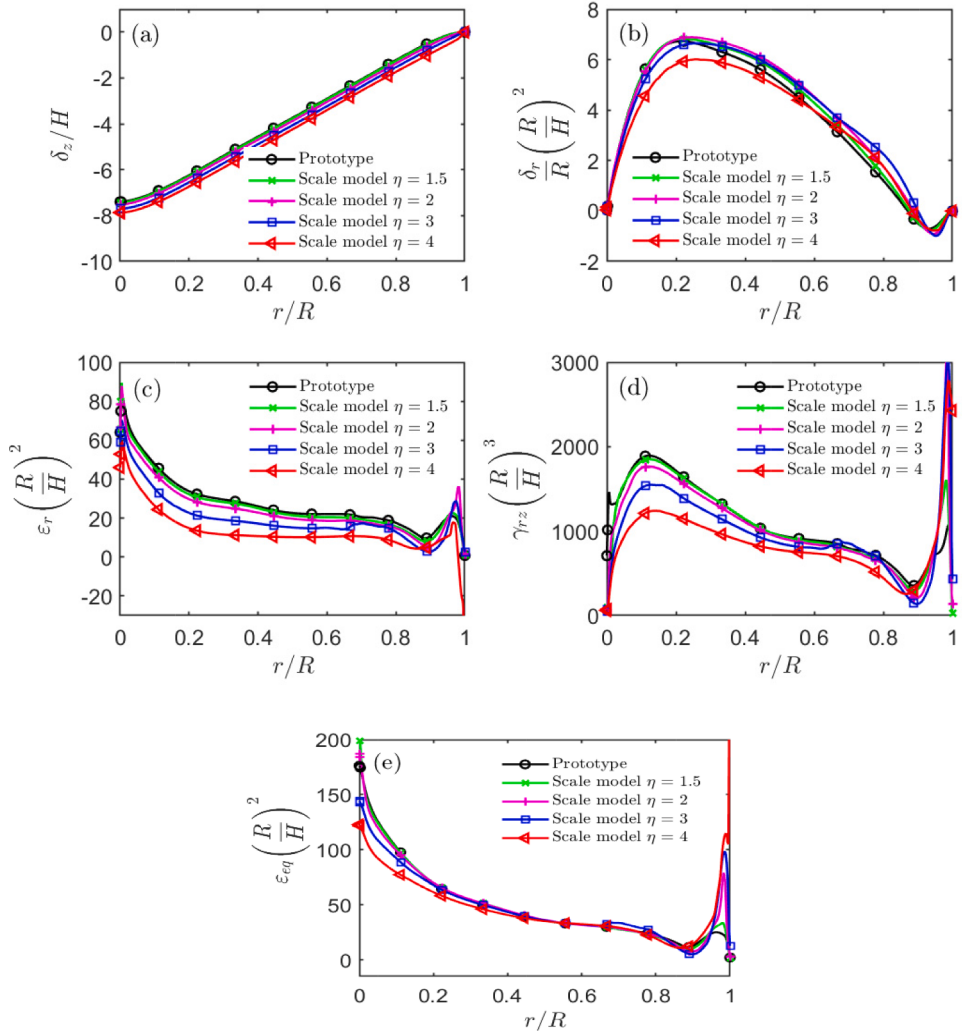


Fig. 8. The similarity of deformation fields on the neutral plane for circular plates at final time $tV_0/H = 8$ (Loading case II).

transverse normal on neutral plane for the four scaled models $\eta = 1.5, 2, 3$ and 4 are obtained as $1.03^\circ, 1.51^\circ, 2.02^\circ, 2.98^\circ$ and 3.98° , respectively. Therefore, the larger the geometric distortion degree η , the larger the relative deformation of the scaled model. When the numbers $\Pi_{\delta_z} = \frac{\delta_z}{L_z}$

and $\Pi_{\delta_r} = \frac{\delta_r}{R} \left(\frac{R}{L_z} \right)^2$ are used to regularize the structural response, the dimensionless displacement fields of scaled models show good consistency with those of prototype on whole spatial field, Fig. 4b and d. Meanwhile, the different powers, $n = 0$ and 2 , for the ratio of characteristic lengths, \bar{R}/\bar{L}_z , are verified. The perfect similarity of Π_{δ_r} also verifies reasonableness of the oriented dimension $\dim(\delta_x) = \dim(\delta'_x) = \mathbb{L}_x^{-1} \mathbb{L}_z^2$ in Section 2.2.

(2) Strain

The similarity of strain on the neutral plane at the final time is plotted in Fig. 5. The strain components $\varepsilon_r, \varepsilon_\theta, \varepsilon_z, \gamma_{rz}$ and the equivalent strain ε_{eq} between the prototype and the scaled models show significant difference along the dimensionless spatial positions of $\Pi_r = \frac{r}{R}$, Fig. 5a, c, e, g and l. When the numbers $\Pi_{\varepsilon_r} = \varepsilon_r \left(\frac{R}{L_z} \right)^2$, $\Pi_{\varepsilon_\theta} = \varepsilon_\theta \left(\frac{R}{L_z} \right)^2$, $\Pi_{\varepsilon_z}^{mod} = \varepsilon_z \left(\frac{R}{L_z} \right)^2$, $\Pi_{\gamma_{rz}}^{mod} = \gamma_{rz} \left(\frac{R}{L_z} \right)^3$ and $\Pi_{\varepsilon_{eq}} = \varepsilon_{eq} \left(\frac{R}{L_z} \right)^2$ are used to regularize structural responses, the dimensionless strain distribution of the scaled

models show good consistency with those of the prototype, as expected in Fig. 5b, d, f, h and m. Meanwhile, the different powers, $n = 2$ and 3 , for the ratio of characteristic lengths, \bar{R}/\bar{L}_z , are verified and they are perfectly coupled together in the similarity of $\Pi_{\varepsilon_{eq}}$. Recall that, the transverse shear strains are actually ignored in the equivalent strain ε_{eq} in Section 2.2, while keeping the other strain components. Since the equivalent strain show the good similarity in Fig. 5m, the number $\Pi_{\varepsilon_{eq}}$ is still accurate enough when containing some effects of γ_{rz} in Loading case I.

(3) Stress

The similarity of stress on the neutral plane at time $tV_0/H = 1.2$ is plotted in Fig. 6. The dimensionless stress distribution $\Pi_{\sigma_r} = \frac{\sigma_r}{\rho V_z^2} \left(\frac{L_z}{R} \right)^2$, $\Pi_{\sigma_\theta} = \frac{\sigma_\theta}{\rho V_z^2} \left(\frac{L_z}{R} \right)^2$, $\Pi_{\sigma_z} = \frac{\sigma_z}{\rho V_z^2}$ and $\Pi_{\tau_{rz}} = \frac{\tau_{rz}}{\rho V_z^2} \left(\frac{L_z}{R} \right)$ of the scaled models show good consistency with those of the prototype in Fig. 6a, b, c and d. Meanwhile, the different powers, $n = 0, 1$ and 2 , for the ratio of characteristic lengths, \bar{R}/\bar{L}_z , are verified. In addition, on the neutral plane of $\Pi_r = \frac{r}{R} = \frac{1}{2}$, the ratios σ_z/σ_r and τ_{rz}/σ_r for large distortion of $\eta = 4$ can be obtained as about 0.01 and 0.16 , which indicates that the transverse shear stress τ_{rz} is small and the transverse normal stress is minor. Therefore, it is reasonable to ignore the transverse stress components in

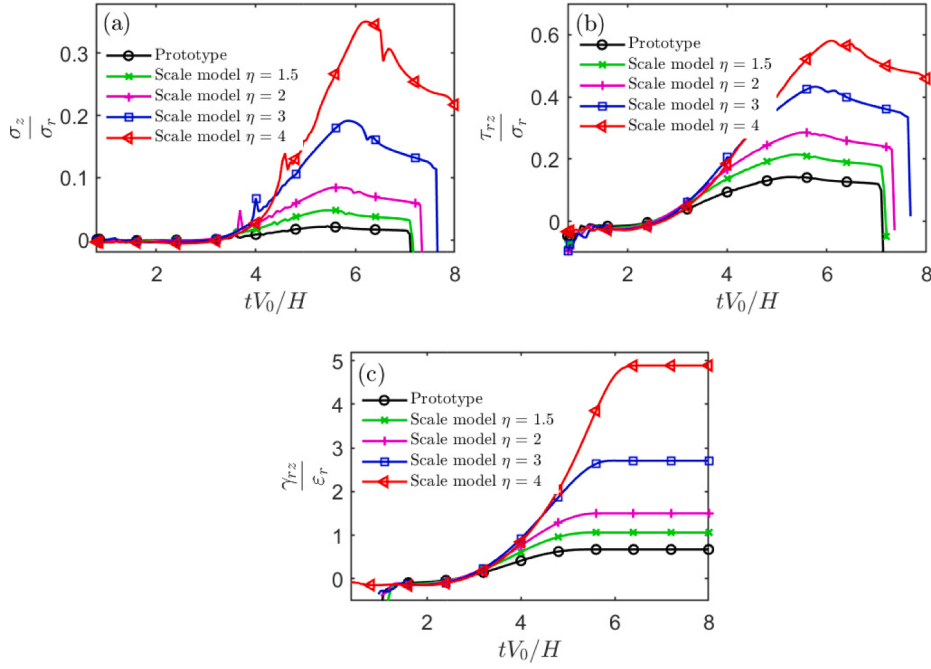


Fig. 9. The stress and strain ratios on the neutral plane spatial positions of $\Pi_r = \frac{r}{R} = \frac{1}{2}$ during deformation history for circular plates (Loading case II).

the oriented dimensional analysis in Section 2.2.

(4) Time-scale analysis

The similarity of $\Pi_t = tV_z/\bar{L}_z$ in temporal fields is evaluated by the four physical quantities δ_z , σ_{eq} , ε_{eq} and $\dot{\varepsilon}_{eq}$, with results plotted in Fig. 7. The dimensionless deflection $\Pi_{\delta_z} = \frac{\delta_z}{\bar{L}_z}$ shows good consistency during whole dimensionless time history, and results in the maximum value about $(\delta_z/H)_{max} = 1.12$ at final time $tV_0/H = 1.344$ in Fig. 7a. For dimensionless equivalent stress $\Pi_{\sigma_{eq}} = \frac{\sigma_{eq}}{\rho V_z^2} \left(\frac{\bar{L}_z}{R} \right)^2$, Fig. 7b shows basically identical similarity, especially in the plastic stage where the scaled model and the prototype are exactly the same. For dimensionless equivalent strain $\Pi_{\varepsilon_{eq}} = \varepsilon_{eq} \left(\frac{\bar{R}}{\bar{L}_z} \right)^2$ and dimensionless equivalent strain rate $\Pi_{\dot{\varepsilon}_{eq}} = \frac{\dot{\varepsilon}_{eq} \bar{L}_z}{V_z} \left(\frac{\bar{R}}{\bar{L}_z} \right)^2$, the deviations are very small, as shown in Fig. 7c and d. In addition, some significant deviation can be found in the initial elastic stage and the time of entering plasticity is advanced with the increase of η , as shown in Fig. 7b. The main reason is that the geometric distortion (usually $\eta > 1$ in scaling tests) of ODLV breaks strain invariability of the traditional similarity laws and makes the scaled model with the large distortion have larger strain responses.

- **Loading Case II**

The refined similarities have been verified in the small degree of deformation of Loading case I. For a larger degree of deformation, the applicability of ODLV need to be evaluated by Loading case II.

(1) Similarity evaluation

The similarity of deformation fields on the neutral plane is evaluated by δ_z , δ_r , ε_r , γ_{rz} and ε_{eq} , with the results plotted in Fig. 8. Some obvious deviations for the distortion of $\eta = 3$ and 4 can be found, while the distortion of $\eta = 1$ and 2 show good consistency. Compared with

Loading case I, the maximum final dimensionless displacements are shown to be significantly increased, from $\frac{\delta_z}{\bar{L}_z} = 1.1$ and $\frac{\delta_r}{\bar{R}} \left(\frac{\bar{R}}{\bar{L}_z} \right)^2 = 0.28$ (Fig. 4b and d) to $\frac{\delta_z}{\bar{L}_z} = 8.0$ and $\frac{\delta_r}{\bar{R}} \left(\frac{\bar{R}}{\bar{L}_z} \right)^2 = 6.9$ (Fig. 8a and b); the maximum dimensionless equivalent strain at circular plate center is increased by as much as 60-fold, from $\varepsilon_{eq} \left(\frac{\bar{R}}{\bar{L}_z} \right)^2 = 3.4$ (Fig. 5m) to $\varepsilon_{eq} \left(\frac{\bar{R}}{\bar{L}_z} \right)^2 = 200$ (Fig. 8e). For the large deformations of Loading case II, the extent of these deviations can be considered small and generally acceptable. In addition, for the prototype and the four scaled models, the maximum normal strains along r -axis at the center point (see Fig. 8c) and the maximum transverse shear strains near the root (see Fig. 8d) are $\varepsilon_r = 0.02, 0.05, 0.09, 0.16, 0.24$ and $\gamma_{rz} = 0.004, 0.022, 0.10, 0.34, 0.73$, respectively. Therefore, the scaled model with large distortion η is more prone to fracture following the plasticity due to large strain responses.

The similarities of other physical quantities are similar to the analysis results in Fig. 8 in which some obvious deviations can be observed, especially for the distortion of $\eta = 3$ and 4. For limited space, it will not be shown here.

(2) Deviation analysis

Some evident deviations existed in Loading case II can be attributed to the transverse stresses σ_z , τ_{rz} and the transverse strain γ_{rz} since they are usually neglected for the thin-plate impact problem in Section 2.2. In order to evaluate their influence, the ratios σ_z/σ_r , τ_{rz}/σ_r and $\gamma_{rz}/\varepsilon_r$ on the neutral plane of $\Pi_r = \frac{r}{R} = \frac{1}{2}$ are plotted in Fig. 9. It is evident that σ_z/σ_r , τ_{rz}/σ_r and $\gamma_{rz}/\varepsilon_r$ increases significantly with the increase of deformation, especially for the distortion of $\eta = 3, 4$. The final dimensionless response time also increases as the distortion η increases. Obviously, the transverse stresses σ_z and τ_{rz} and the transverse strain γ_{rz} play an important role in Loading case II and therefore cannot be neglected, especially for the distortion of $\eta = 3$ and 4.

Since the shear strain cannot be ignored, the geometric nonlinearity assumption of small strains with moderate rotation ($10^\circ - 15^\circ$) should be

further examined. The rotations of transverse normal on neutral plane for the prototype and the four scaled models are respectively obtained as 6.8°, 10.0°, 13.5°, 20.2° and 26.7°, according to the arctangent of $(\delta_z)_{max}/R$ in Fig. 8a. Apparently, the prototype and the scaled models of $\eta = 1.5$ and 2 are in the scope of medium rotation, while the scaled models of $\eta = 3$ and 4 with larger deformation are out of the scope of moderate rotations. That explains why the similarity results of distortion of $\eta = 1.5$ and 2 are much better than the distortion of $\eta = 3$ and 4 in Loading case II.

The above refined analyses show that, when the ODLV numbers are used to regularize the geometrically distorted structures, the structural plastic responses for both direction-dependent and direction-independent physical quantities all show good similarity on both spatial and temporal fields in the geometric nonlinearity assumption of small strains under moderate rotation of 10° – 15°.

5. Conclusions

A directional framework of similarity laws, called ODLV (oriented-density-length-velocity), for the geometrically distorted structures subjected to impact loading is presented here. Since the structural characteristic lengths in three spatial directions are systematically introduced into dimensional and similarity analysis, it can be considered as a substantive progress for similarity laws of solid mechanics. Compared with previous dimensional analysis systems such as MLT, VSG, VSM and DLV, six main aspects are reflected.

- (1) The oriented dimensions of twenty-eight basic physical quantities, based on the thin-plate impact problem, are defined to establish the theoretical foundation of dimensional analysis. The dimensionless numbers of spatial directions and their corresponding scaling factors are comprehensively proposed by the oriented-density-length-velocity (ODLV) dimensional analysis. In addition to the main study object of rigid-plastic materials, the proposed framework is also applicable to anisotropic elastic materials, as proved in Appendix A.
- (2) Three directional characteristic lengths \bar{L}_x , \bar{L}_y and \bar{L}_z in the Cartesian coordinate system (or \bar{L}_r , \bar{L}_θ and \bar{L}_z in the cylindrical coordinate system) are used instead of the only one scalar characteristic length \bar{L} in the previous similarity laws. The different powers (e.g., $n = 0, 1, 2, 3$) of the ratios of the undistorted characteristic lengths to the distorted characteristic lengths (e.g., \bar{L}_x/\bar{L}_z , \bar{L}_y/\bar{L}_z) naturally express the geometrically distorted similarity laws of different directional physical quantities. Meanwhile, these different powers can be coupled to the equivalent stress and the equivalent strain to control the similarity law of rigid-plastic structures.
- (3) Three correction methods of impact velocity, density (or structural mass and impact mass) and geometrical thickness are proposed to address the geometric distortion as well as the distortion

of different materials (including strain hardening and strain rate effects) and gravity effects, which can be used in separation or in combination.

- (4) Various dimensionless response equations about transverse displacement, rotation angle, time, equivalent strain and equivalent strain rate for different types of impacted structures are concisely, clearly and perfectly expressed by the proposed dimensionless numbers.
- (5) The scaling analysis ability for geometrically distorted structures is verified. For the relatively simple analytical models of impacted beams under the condition of finite displacements, exact similarity can be obtained. For the refined numerical model of an impacted circular plate, very good similarity can also be further obtained for the directional components of displacement, stress and strain in both spatial and temporal fields in the case of the geometric nonlinearity with small strains but moderate rotation.

Since the presented framework is based on the thin-plate assumptions, more complex structures and situations are required to be verified and studied in the future.

CRediT authorship contribution statement

Shuai Wang: Conceptualization, Methodology, Formal analysis, Writing, Visualization, Supervision; Fei Xu: Methodology, Supervision, Writing – review & editing, Critical revisions, Funding acquisition, Resources; Xiaoyu Zhang: Critical revisions, Writing – review & editing, Software; Zhen Dai: Investigation, Validation; Xiaochuan Liu, Validation; Chunyu Bai: Validation.

Declaration of Competing Interest

The authors declare that they have no known competing financial interests or personal relationships that could have appeared to influence the work reported in this paper.

Acknowledgements

Preprint services of [preprints.org](https://www.preprints.org) for sharing our not peer-reviewed manuscript at 25 February 2020 (<https://www.preprints.org/manuscript/202002.0394/v1>) is gratefully acknowledged.

Useful discussions with Mr. Wanlin Guo (Nanjing University of Aeronautics and Astronautics, Nanjing 210016, China), Mr. Chao Zhang and Miss Muqiu Hu (Northwestern Polytechnical University, Xi'an 710072, Shaanxi, China) are gratefully acknowledged. This work is supported by the National Nature Science Foundations of China [grant no. 11972309]; and the Overseas Expertise Introduction Project for Discipline Innovation (the 111 Project) [grant no. BP0719007].

Appendix A

For the orthotropic elastic materials, the generalized Hooke's law [39] is considered as

$$\left. \begin{aligned} \epsilon_x &= \frac{\sigma_x}{E_x} - \nu_{yx}\frac{\sigma_y}{E_y} - \nu_{zx}\frac{\sigma_z}{E_z}, & \epsilon_y &= \frac{\sigma_y}{E_y} - \nu_{zy}\frac{\sigma_z}{E_z} - \nu_{xy}\frac{\sigma_x}{E_x}, \\ \epsilon_z &= \frac{\sigma_z}{E_z} - \nu_{xz}\frac{\sigma_x}{E_x} - \nu_{yz}\frac{\sigma_y}{E_y}, & \gamma_{xy} &= \frac{\tau_{xy}}{E_{xy}}, & \gamma_{xz} &= \frac{\tau_{xz}}{E_{xz}}, & \gamma_{yz} &= \frac{\tau_{yz}}{E_{yz}} \end{aligned} \right\}, \quad (\text{A.1})$$

where $\nu_{ij} = \frac{|\epsilon_j|}{|\epsilon_i|}$ is Poisson's ratio; and $i, j = x, y, z$.

The oriented relations for Eq. (A.1) can be obtained as

$$\dim(\nu_{ij}) = \frac{\dim(\varepsilon_j)}{\dim(\varepsilon_i)}, \dim(E_{ij}) = \frac{\dim(\sigma_{ij})}{\dim(\varepsilon_{ij})} \quad (\text{no sum on } i,j); \quad (\text{A.2})$$

Therefore, the oriented dimensions of ν_{ij} and E_{ij} at the different spatial directions are only related to the stress and strain of the related directions. By combining $\Pi_{\sigma_{ij}}$ (Eq. (11a)) and $\Pi_{\varepsilon_{ij}}$ (Eq. (11b)), the dimensionless numbers of ν_{ij} and E_{ij} can be directly obtained as

$$\Pi_{\nu_{ij}} = \left[\nu_{ij} \left(\frac{\bar{L}_j}{\bar{L}_i} \right)^2 \right], \Pi_{E_{ij}} = \left[\frac{\rho V_0^2}{E_{ij}} \left(\frac{\sqrt{\bar{L}_i \bar{L}_j}}{\bar{L}_z} \right)^4 \right] \quad (\text{no sum on } i,j); \quad (\text{A.3})$$

It should be noted that the numbers $\Pi_{E_{ij}}$ can be explained as the important form of the well-known Zhao's response number, $R_n (n = 0, 2, 4) = \frac{\rho V_0^2}{E} \left(\frac{\bar{L}}{H} \right)^n$. The exponents $n = 0, 2, 4$ are derived.

The above analysis indicates that $\Pi_{\sigma_{ij}}$ and $\Pi_{\varepsilon_{ij}}$ are perfectly applicable to the stress-strain relationship of orthotropic elastic materials. Compared with the isotropic rigid-plastic materials in Eq. (3) requiring that the x-y plane is isotropic, the characteristic lengths \bar{L}_x, \bar{L}_y and \bar{L}_z are independent of each other here.

Appendix B

- For the cantilever beam subjected to mass impact [43], Fig. 2a, the maximum permanent transverse displacement (W_f) at the mid-span is given as

$$W_f = \frac{\mu V_0^2 l^2 \kappa^2}{3\Psi_0} \left[\frac{1}{1+2\kappa} + 2\ln\left(1+\frac{1}{2\kappa}\right) \right], \quad (\text{B.1a})$$

where $\mu = \rho BH$ is the mass per unit length; B is width of beams; $\kappa = G/\mu l = G/2\rho LBH$ is the mass ratio of impact mass to structure mass; and $\Psi_0 = \sigma_d BH^2/4$ is fully plastic bending moment.

The final rotation angle (α_f) at the root and is given as

$$\alpha_f = \frac{\mu l V_0^2}{6\Psi_0} (1+3\kappa) \left(1 + \frac{1}{2\kappa}\right)^{-2}. \quad (\text{B.1b})$$

The final response time (T_f) is given as

$$T_f = \frac{GV_0 l}{\Psi_0}. \quad (\text{B.1c})$$

- For the clamped beam subjected to impact mass [44], Fig. 2b, the maximum permanent transverse displacement (W_f) at the mid-span is given as

$$\frac{W_f}{H} = \frac{1}{2} \left[\left(1 + \frac{2GV_0^2 L}{BH^3 \sigma_d} \right)^{1/2} - 1 \right], \quad (\text{B.2a})$$

where the effects of finite displacements have been taken into account.

The equivalent strain is given as [45]

$$\varepsilon_{eq} = \begin{cases} \sqrt{\left(3 \frac{W_f H}{L^2} \right)^2 + \left(\frac{4c}{\sqrt{3}} \frac{W_f}{L} \right)^2}, & \text{for } \frac{W_f}{H} \leq 1 \\ \sqrt{\left\{ \frac{1}{2} \left(\frac{H}{L} \right)^2 \left[\left(\frac{W_f}{H} \right)^2 + 5 \right] \right\}^2 + \left(\frac{4c}{\sqrt{3}} \frac{W_f}{L} \right)^2}, & \text{for } \frac{W_f}{H} > 1 \end{cases}, \quad (\text{B.2b})$$

where c is dimensional constant. Inside the two square roots on the right-hand of Eq. (B.2b), the first terms introduce the membrane strain and the bending strain; and the second terms introduce the transverse shear strain.

- For the clamped beam subjected to impulsive velocity [6], Fig. 2c, the maximum permanent transverse displacement (W_f) at the mid-span is given as

$$\frac{W_f}{H} = \frac{1}{2} \left[\left(1 + \frac{3\rho V_0^2 L^2}{\sigma_d H^2} \right)^{1/2} - 1 \right]. \quad (\text{B.3a})$$

where the effects of finite displacements have been taken into account.

And the average of equivalent strain rate is considered as

$$\dot{\epsilon}_{eq} = \frac{V_0 W_f}{3\sqrt{2}L^2}. \quad (\text{B.3b})$$

Appendix C

A simple or clamp supported rectangular plate subjected to impact mass is shown in Fig. C. The impact models of plate are assumed to be of the rigid-plastic materials and take into account the effects of finite displacements.

The maximum permanent transverse displacements (W_f) are given as [46]

$$\frac{W_f}{H} = \frac{(1+\omega)}{2} \left[\sqrt{1 + \frac{12\zeta\Omega\kappa(1+6\kappa)}{(1+\zeta^2)(1+\omega)^2(1+3\kappa)^2}} - 1 \right] \quad (\text{C.1})$$

where $\zeta = \frac{B}{L}$; $\Omega = \frac{GV_0^2}{4\sigma_d H^3}$; $\kappa = G/[\mu'(2L)(2B)]$ is mass ratios; $\mu' = \rho H$ is mass per unit surface area; and ω is dimensionless moment resistance at supports ($\omega = 0$ and 1 for simply and fully clamped supports, respectively).

When the structural geometric characteristics are considered by the directional characteristic lengths L , B and H , Eq. (C.1) can be re-expressed as

$$\frac{W_f}{H} = \frac{(1+\omega)}{2} \left\{ \sqrt{1 + \frac{\rho V_0^2 (L/H)^2}{\sigma_d} \frac{3\zeta^2 \kappa^2 (1+6\kappa)}{(1+\zeta^2)(1+\omega)^2(1+3\kappa)^2}} - 1 \right\}. \quad (\text{C.2})$$

which shows the relation between the three independent dimensionless input variables, $\left[\frac{\rho V_0^2}{\sigma_d} \left(\frac{L}{H} \right)^2 \right]$, $\left[\frac{G}{\rho L B H} \right]$ and $\left[\frac{B}{L} \right]$, and the one independent dimensionless output variable, $\left[\frac{W_f}{H} \right]$, for response equation of the impacted plate. The number $\left[\frac{B}{L} \right]$ (or $\Pi_\zeta = \left[\frac{L_x}{L_y} \right]$) represents a dimensionless expression for the isotropic relation L_x/L_y . Obviously, except for the number $\Pi_\zeta = \left[\frac{L_x}{L_y} \right]$, the dimensionless response equation of plate (high-dimensional structure) is similar to one-dimensional beams of Eqs. (15a) and (16a). The excellent performances of the ODLV for expressing various dimensionless response equations are verified again.

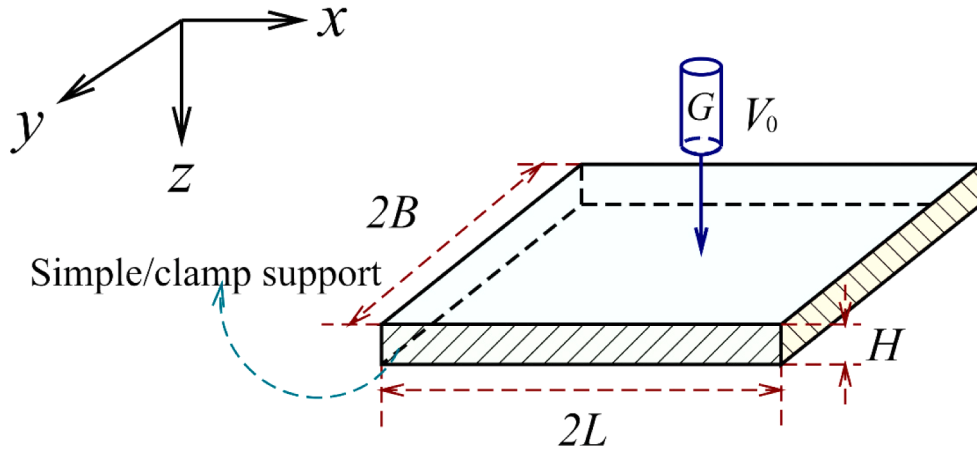


Fig. C. A simple or clamp supported rectangular plate subjected to impact mass.

Appendix D

In order to more intuitively show the similarity of geometric distortion considering the material strain hardening and strain rate effects, the Johnson-Cook constitutive model is further used to verify the numerical model of the Loading case II in Section 4.1. The Johnson-Cook equation [42] is expressed as

$$\sigma_d = (A_1 + A_2 \epsilon^n)(1 + A_3 \ln(\dot{\epsilon} / \dot{\epsilon}_0)), \quad (\text{D.1})$$

Table D.1

Material parameters for the Johnson–Cook constitutive equation.

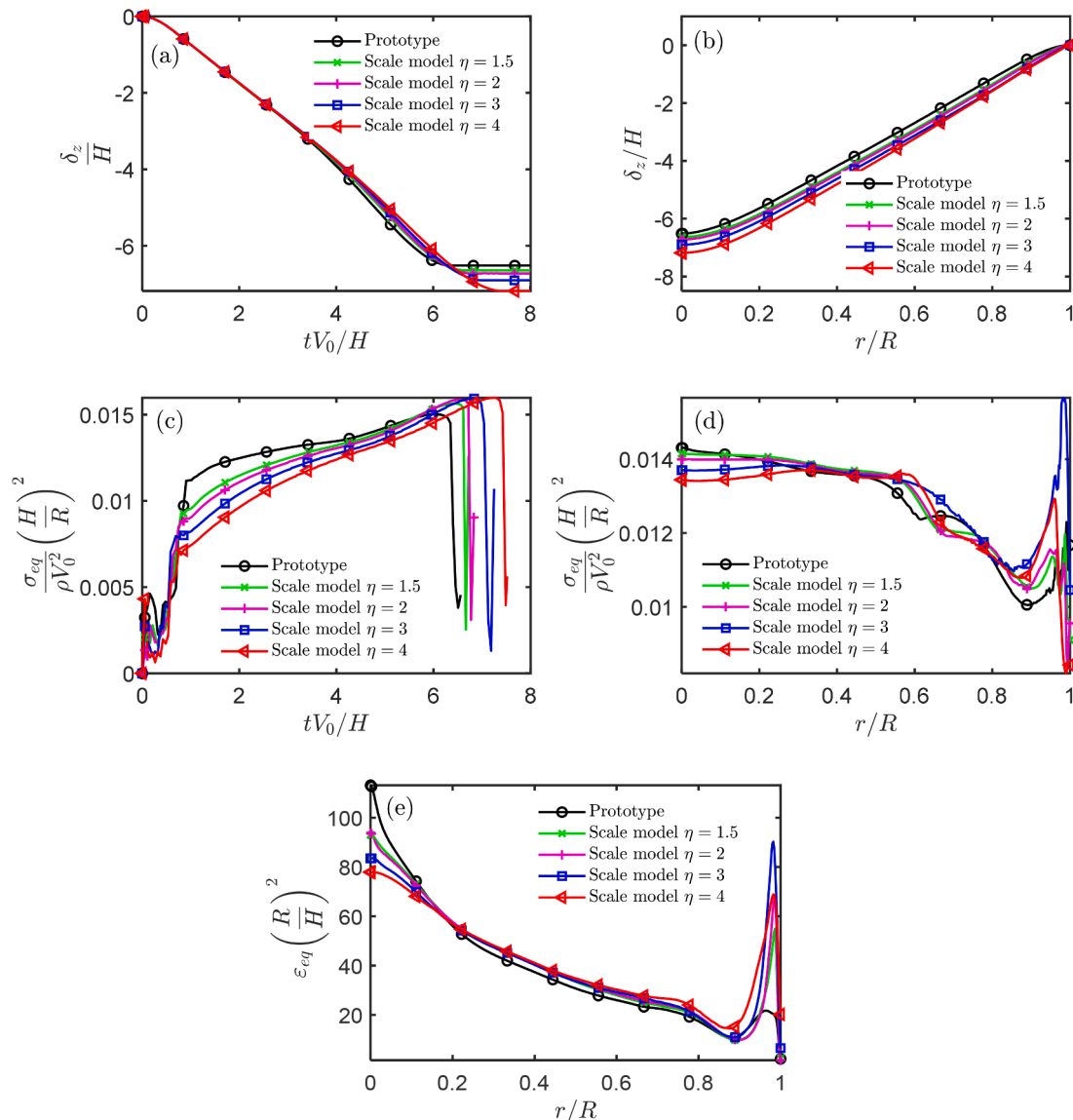
Material	Density [kg/m ³]	Elastic modulus[GPa]	Poisson's Ratio	A ₁ [MPa]	A ₂ [MPa]	n	A ₃	$\dot{\epsilon}_0$ [s ⁻¹]
1006 Steel	7.89E3	200	0.30	350	275	0.360	0.022	1
Aluminium 2024	2.70E3	72.4	0.33	265	426	0.340	0.015	1

Table D.2

Scaling factors of input parameters for circular plates with the Johnson-Cook equation.

Factor	Prototype	Model $\eta = 1.5$	Model $\eta = 2.0$	Model $\eta = 3.0$	Model $\eta = 4.0$
β_ρ	1	0.342	0.342	0.342	0.342
β_{V_z}	1	2.51	3.47	5.50	7.67
β_t	1	0.0598	0.0576	0.0545	0.0522
β_{P_z}	1	2.16	4.12	10.35	20.13

where A_1 is quasi-static flow stress; A_2 , A_3 and n are material constants; $\dot{\epsilon}_0$ is reference strain-rate. Two completely different materials, 1006 Steel and Aluminium 2024, are used to design prototype and scaled model, respectively. The material parameters [42] are shown in Table D.1. In addition, the velocity correction factor β_{V_z} can be obtained from Eq. (14). The average strain and the average strain rate [47] used for Eq. (14) are approximated by $\bar{\epsilon}_p = \frac{\rho V_0^2}{3\sigma_0} = 0.0077$ and $\bar{\dot{\epsilon}}_p = \frac{4\sqrt{2V_0^2}}{\sqrt{3}\pi R} \sqrt{\frac{\rho}{\sigma_0}} = 40.43 \text{ s}^{-1}$, respectively. Then, the scaling factors β_ρ , β_{V_z} , β_t and β_{P_z} are listed in Table D.2. Other scaling factors

**Fig. D.** Similarity of center point and neutral plane for circular plates (Loading case II and the Johnson-Cook equation).

and the numerical modeling methods are exactly the same as in [Section 4.1.1](#).

For different materials with strain hardening and strain rate effects, the similarity of geometric distortion in temporal and spatial fields is evaluated by the three physical quantities δ_z , σ_{eq} and ε_{eq} , with results plotted in [Fig. D.1](#). Compared with the Loading case II with the rigid-perfectly plastic model in [Section 4.1.2](#), the similarity error of these physical quantities is not large and can be considered generally acceptable. In addition, different from the completely exact similarity of the equivalent stress in [Section 4.1](#), the significant error can be observed from [Fig. Dc](#) and [Dd](#). This is mainly caused by the fact that the correction factor β_{V_z} is associated with the constitutive parameters and cannot exactly satisfy [Eq. \(13\)](#) when the general constitutive relation is used.

References

- [1] Simites GJ, Rezaeepazhand J. Structural similitude and scaling laws for laminated beam plates. National Aeronautics and Space Administration; 1992. Technical Report NASA CR-190585.
- [2] Coutinho CP, Baptista AJ, Rodrigues JD. Reduced scale models based on similitude theory: A review up to 2015. *Engineering Struct* 2016;119:81–94. <https://doi.org/10.1016/j.engstruct.2016.04.016>.
- [3] Casaburo A, Petrone P, Franco F, Rosa SD. A Review of Similitude Methods for Structural Engineering. *Appl. Mech. Rev.* 2019;71(3):030802. <https://doi.org/10.1115/1.4043787>.
- [4] Zohuri B. Dimensional analysis and self-similarity methods for engineers and scientists. Springer; 2015.
- [5] Davey K, Darvizeh R, Al-Tamimi A. Scaled metal forming experiments: A transport equation approach. *Int. J. Solids Struct.* 2017;125:184–205. <https://doi.org/10.1016/j.ijsolstr.2017.07.006>.
- [6] Jones N. Structural impact. Cambridge: Cambridge University Press; 1989.
- [7] Lu G, Yu TX. Energy absorption of structures and materials. Cambridge: Cambridge Woodhead Publishing; 2003.
- [8] Booth E, Collier D, Miles J. Impact scalability of plated steel structures. In: Jones N, Wierzbicki T, editors. Structural Crashworthiness. Butterworks, London; 1983. p. 136–74.
- [9] Jones N, Jouri W, Birch R. On the scaling of ship collision damage, International Maritime Association of the East Mediterranean. Third International Congress on Marine Technology, Athens 1984;2:287–94.
- [10] Wen HM, Jones N. Experimental investigation of the scaling laws for metal plates struck by large masses. *Int. J. Impact Eng.* 1993;13:485–505. [https://doi.org/10.1016/0734-743X\(93\)90120-V](https://doi.org/10.1016/0734-743X(93)90120-V).
- [11] Jiang P, Wang W, Zhang GJ. Size effects in the axial tearing of circular tubes during quasi-static and impact loadings. *Int. J. Impact Eng.* 2006;32:2048–65. <https://doi.org/10.1016/j.ijimpeng.2005.07.001>.
- [12] Fu S, Gao X, Chen X. The similarity law and its verification of cylindrical lattice shell model under internal explosion. *Int. J. Impact Eng.* 2018;122:38–49. <https://doi.org/10.1016/j.ijimpeng.2018.08.010>.
- [13] Drazetic P, Ravalard Y, Dacheux F, Marguet B. Applying non-direct similitude technique to the dynamic bending collapse of rectangular section tubes. *Int. J. Impact Eng.* 1994;15:797–814. [https://doi.org/10.1016/0734-743X\(94\)90066-T](https://doi.org/10.1016/0734-743X(94)90066-T).
- [14] Oshiro RE, Alves M. Scaling impacted structures. *Arch. Appl. Mech.* 2004;74:130–45. <https://doi.org/10.1007/s00419-004-0343-8>.
- [15] Oshiro RE, Alves M. Scaling of cylindrical shells under axial impact. *Int. J. Impact Eng.* 2007;34:89–103. <https://doi.org/10.1016/j.ijimpeng.2006.02.003>.
- [16] Oshiro RE, Alves M. Scaling of structures subject to impact loads when using a power law constitutive equation. *Int. J. Solids Struct.* 2009;46:3412–21. <https://doi.org/10.1016/j.ijsolstr.2009.05.014>.
- [17] Mazzariol LM, Oshiro RE, Alves M. A method to represent impacted structures using scaled models made of different materials. *Int. J. Impact Eng.* 2016;90:81–94. <https://doi.org/10.1016/j.ijimpeng.2015.11.018>.
- [18] Alves M, Oshiro RE. Scaling impacted structures when the prototype and the model are made of different materials. *Int. J. Solids Struct.* 2006;43:2744–60. <https://doi.org/10.1016/j.ijsolstr.2005.03.003>.
- [19] Wei D, Hu C. Scaling of an impacted reticulated dome using partial similitude method. *Lat. Am. J. Solids Struct.* 2019;16:e158. <https://doi.org/10.1590/1679-78255342>.
- [20] Wang S, Xu F, Dai Z, et al. A direct scaling method for the distortion problems of structural impact. *Chinese Journal of Theoretical and Applied Mechanics* 2020;52:774–86. [\(in Chinese\).](https://doi.org/10.6052/0459-1879-19-327)
- [21] Jiang ZR, Zhong YK, Shi KR, Luo B. Gravity-based impact comparability rule of single-layer reticulated shells and its numerical verification. *J. South China Univ. Techno. (Nat. Sci. Ed.)* 2016;44:43–8. [\(in Chinese\).](https://doi.org/10.3969/j.issn.1000-565X.2016.10.007)
- [22] Sadeghi H, Davey K, Darvizeh R, Darvizeh A. A scaled framework for strain rate sensitive structures subjected to high rate impact loading. *Int. J. Impact Eng.* 2019;125:229–45. <https://doi.org/10.1016/j.ijimpeng.2018.11.008>.
- [23] Sadeghi H, Davey K, Darvizeh R, Darvizeh A. Scaled models for failure under impact loading. *Int. J. Impact Eng.* 2019;129:36–56. <https://doi.org/10.1016/j.ijimpeng.2019.02.010>.
- [24] Sadeghi H, Alitavoli M, Darvizeh A, Rajabiehfard R. Dynamic plastic behaviour of strain rate sensitive tubes under axial impact. *Thin Wall. Struct.* 2019;143:106220. <https://doi.org/10.1016/j.tws.2019.106220>.
- [25] Oshiro RE, Alves M. Predicting the behaviour of structures under impact loads using geometrically distorted scaled models. *J. Mech. Phys. Solids* 2012;60:1330–49. <https://doi.org/10.1016/j.jmps.2012.03.005>.
- [26] Kong XS, Li X, Zheng C, Liu F, We WG. Similarity considerations for scale-down model versus prototype on impact response of plates under blast loads. *Int. J. Impact Eng.* 2017;101:32–41. <https://doi.org/10.1016/j.ijimpeng.2016.11.006>.
- [27] Mazzariol LM, Alves M. Similarity laws of structures under impact load: Geometric and material distortion. *Int. J. Mech. Sci.* 2019;157:158:633–47. <https://doi.org/10.1016/j.ijmecsci.2019.05.011>.
- [28] Mazzariol LM, Alves M. Experimental verification of similarity laws for impacted structures made of different materials. *Int. J. Impact Eng.* 2019;133:103364. <https://doi.org/10.1016/j.ijimpeng.2019.103364>.
- [29] Wang S, Xu F, Dai Z. Suggestion of the DLV dimensionless number system to represent the scaled behavior of structures under impact loads. *Arch. Appl. Mech.* 2020;90:707–19. <https://doi.org/10.1007/s00419-019-01635-9>.
- [30] Johnson W. Impact strength of materials. London: Edward Arnold; 1972.
- [31] Zhao YP. Prediction of structural dynamic plastic shear failure by Johnson's damage number. *Fortsch. Ingenieurwes.* 1998;63:349–52. <https://doi.org/10.1007/PL000010753>.
- [32] Zhao YP. Suggestion of a new dimensionless number for dynamic plastic response of beams and plates. *Arch. Appl. Mech.* 1998;68:524–38. <https://doi.org/10.1007/s004190050184>.
- [33] Zhao YP. Similarity consideration of structural bifurcation buckling. *Fortsch. Ingenieurwes.* 1999;65:107–12. <https://doi.org/10.1007/PL000010868>.
- [34] Shi XH, Gao YG. Generalization of response number for dynamic plastic response of shells subjected to impulsive loading. *Int. J. Pressure Vessels Piping* 2001;78:453–9. [https://doi.org/10.1016/S0308-0161\(01\)00050-3](https://doi.org/10.1016/S0308-0161(01)00050-3).
- [35] Hu YQ. Application of response number for dynamic plastic response of plates subjected to impulsive loading. *Int. J. Pressure Vessels Piping* 2000;77:711–4. [https://doi.org/10.1016/S0308-0161\(00\)00082-X](https://doi.org/10.1016/S0308-0161(00)00082-X).
- [36] Hu YQ. Dynamic plastic response of beams subjected to impact of concentrated mass. *J. Nanjing U. Aeronaut. Astronautics* 2009;41:25–9. [\(in Chinese\).](https://doi.org/10.16356/j.1005-2615.2009.01.003)
- [37] Huntley HE. Dimensional analysis. London: MacDonald & Co. Ltd.; 1952.
- [38] Chien WZ. Applied mathematics. Anhui Science and Technology Press. Hefei 1993 (in Chinese).
- [39] Reddy JN. Theory and analysis of elastic plates and shells. Second Edition. CRC Press; Taylor & Francis Group; 2007.
- [40] Yu TX, Xue P. Engineering plastic mechanics. Beijing (in Chinese): China Higher Education Press; 2010.
- [41] Süli E, Mayers DF. An introduction to numerical analysis. New York: Cambridge University Press; 2003.
- [42] Johnson R, Cook WK. A constitutive model and data for metals subjected to large strains high strain rates and high temperatures. In: The 7th International Symposium on Ballistics. The Hague; 1983. p. 541–7.
- [43] Yu TX, Qiu XM. Introduction to Impact Dynamics. Beijing: Tsinghua University Press; 2018.
- [44] Liu JH, Jones N. Dynamic response of a rigid plastic clamped beam struck by a mass at any point on the span. *Int. J. Solids Struct.* 1988;24:251–70. [https://doi.org/10.1016/0020-7683\(88\)90032-7](https://doi.org/10.1016/0020-7683(88)90032-7).
- [45] Alves M, Jones N. Impact failure of beams using damage mechanics: part I—analytical model. *Int. J. Impact Eng.* 2002;27:837–61. [https://doi.org/10.1016/S0734-743X\(02\)00017-9](https://doi.org/10.1016/S0734-743X(02)00017-9).
- [46] Jones N. Impact loading of ductile rectangular plates. *Thin Wall. Struct.* 2012;50:68–75. <https://doi.org/10.1016/j.tws.2011.09.006>.
- [47] Jones N. Dynamic inelastic response of strain rate sensitive ductile plates due to large impact, dynamic pressure and explosive loadings. *Int. J. Impact Eng.* 2014;74:3–15. <https://doi.org/10.1016/j.ijimpeng.2013.05.003>.